WHY LOTTERY TICKET WINS? A THEORETICAL PERSPECTIVE OF SAMPLE COMPLEXITY ON SPARSE NEURAL NETWORKS

Anonymous authors
Paper under double-blind review

ABSTRACT

The *lottery ticket hypothesis* (LTH) (Frankle & Carbin, 2019) states that learning on a properly pruned network (the *winning ticket*) has improved test accuracy over the originally unpruned network. Although LTH has been justified empirically in a broad range of deep neural network (DNN) involved applications like computer vision and natural language processing, the theoretical validation of the improved generalization of a winning ticket remains elusive. To the best of our knowledge, our work, for the first time, characterizes the performance of training a sparse neural network by analyzing the geometric structure of the objective function and the sample complexity to achieve zero generalization error. We show that the convex region near a desirable model with guaranteed generalization enlarges as the neural network model is pruned, indicating the structural importance of a winning ticket. Moreover, as the algorithm for training a sparse neural network is specified as (accelerated) stochastic gradient descent algorithm, we theoretically show that the number of samples required for achieving zero generalization error is proportional to the number of the non-pruned weights in the hidden layer. With a fixed number of samples, training a pruned neural network enjoys a faster convergence rate to the desirable model than training the original unpruned one, providing a formal justification of the improved generalization of the winning ticket. Our theoretical results are acquired from learning a sparse neural network of one hidden layer, while experimental results are further provided to justify the implications in pruning multi-layer neural networks.

1 INTRODUCTION

Neural network pruning can reduce the computational cost of training a model significantly (LeCun et al., 1990; Hassibi & Stork, 1993; Dong et al., 2017; Han et al., 2015; Hu et al., 2016; Srinivas & Babu, 2015; Yang et al., 2017; Molchanov et al., 2017). The recent *Lottery Ticket Hypothesis* (LTH) (Frankle & Carbin, 2019) claims that a randomly initialized dense neural network always contains a so-called "winning ticket," which is a sub-network bundled with the corresponding initialization, such that when trained in isolation, this winning ticket can achieve at least the same testing accuracy as that of the original network by running at most the same amount of training time. This so-called "improved generalization of winning tickets" is verified empirically in (Frankle & Carbin, 2019). LTH has attracted a significant amount of recent research interests (Ramanujan et al., 2020; Zhou et al., 2019; Malach et al., 2020). Despite the empirical success (Evci et al., 2020; You et al., 2019; Wang et al., 2019; Chen et al., 2020a), the theoretical justification of winning tickets are remains elusive expect for a few recent works. Malach et al. (2020) provides the first theoretical evidence that within a randomly initialized neural network, there exists a good sub-network that can achieve the same test performance as the original network. Arora et al. (2018) and Zhou et al. (2018) show that the expressive power of a neural network is comparable to a compressed neural network and both

networks have the same generalization error. However, no theoretical explanation has been provided for the improved generalization of winning tickets, i.e., winning tickets can achieve higher test accuracy after the same training time.

Contributions: This paper provides the *first* systematic analysis of learning sparse neural networks with a finite number of training samples. Our analytical results also provide justification of the LTH from the perspective of the sample complexity. In particular, we provide the *first* theoretical justification of the improved generalization of winning tickets. Specific contributions include:

1. **Sparse neural network learning via accelerated gradient descent (AGD)**: We propose an AGD algorithm with tensor initialization to learn the sparse model from training samples. Considering the scenario where there exists a ground-truth sparse one-hidden-layer neural network, we prove that our algorithm converges to the ground-truth model linearly, which has guaranteed generalization on testing data.

2. **First sample complexity analysis for pruned networks**: We characterize the required number of samples for successful convergence, termed as the *sample complexity*. Our sample complexity depends linearly on the number of the non-pruned weights of the sparse network and is a significant reduction from directly applying conventional complexity bounds in (Zhong et al., 2017; Zhang et al., 2020a;c).

3. **Characterization of the benign optimization landscape of pruned networks**: We show analytically that the empirical risk function has an enlarged convex region near the ground-truth model if the neural network is sparse, justifying the importance of a good sub-network (i.e., the winning ticket).

4. **Characterization of the improved generalization of winning tickets**: We show that gradient-descent methods converge faster to the ground-truth model when the neural network is properly pruned, or equivalently, learning on a pruned network returns a model closer to the ground-truth model with the same number of iterations, indicating the improved generalization of winning tickets.

1.1 Related Work

Winning tickets. Frankle & Carbin (2019) proposes an *Iterative Magnitude Pruning* (IMP) algorithm to obtain the proper sub-network and initialization. IMP and its variations (Frankle et al., 2019a; Renda et al., 2019) succeed in deeper networks like Residual Networks (Resnet)-50 and Bidirectional Encoder Representations from Transformers (BERT) network (Chen et al., 2020b). (Frankle et al., 2019b) shows that IMP succeeds in finding the "winning ticket" if the ticket is stable to stochastic gradient descent noise. In parallel, (Liu et al., 2018) shows numerically that the "winning ticket" initialization does not improve over a random initialization once the correct subnetworks are found, suggesting that the benefit of "winning ticket" mainly comes from the sub-network structures.

Over-parameterized model. When the number of weights in a neural network is much larger than the number of training samples, the landscape of the objective function of the learning problem has no spurious local minima, and first-order algorithms converge to one of the global optima (Livni et al., 2014; Zhang et al., 2016; Soltanolkotabi et al., 2018). However, the global optima is not guaranteed to generalize well on testing data (Yehudai & Shamir, 2019; Zhang et al., 2016).

Model estimation & Generalization analysis. This framework assumes a ground-truth model that maps the input data to the output labels, and the learning objective is to estimate the ground-truth model, which has a generalization guarantee on testing data. The learning problem has intractably many spurious local minina even for one-hidden-layer neural networks (Shamir, 2018; Safran & Shamir, 2018; Zhang et al., 2016). Assuming an infinite number of training samples, (Brutzkus & Globerson, 2017; Du et al., 2018; Tian, 2017) develop learning methods to estimate the ground-truth model. (Fu et al., 2018; Zhong et al., 2017; Zhang et al., 2020a;c) extend to the practical case of a finite number of samples and characterize the sample complexity for successful estimation of the ground-truth model. Because the analysis complexity

explodes when the number of hidden layers increases, all the analytical results about estimating the ground-truth model are limited to one-hidden-layer neural networks, and the input distribution is often assumed to be the standard Gaussian distribution.

1.2 NOTATIONS

Vectors are bold lowercase, matrices and tensors are bold uppercase. Scalars are in normal font, and sets are in calligraphy and blackboard bold font. $\boldsymbol{I}$ and $\boldsymbol{e}_i$ denote the identity matrix and the i-th standard basis vector. $[Z]$ stands for the set of $\{1, 2, \cdots, Z\}$ for any number $\mathbb{N}^+$. In addition, $f(r) = \mathcal{O}(g(r))$ (or $f(r) = \Omega(g(r))$) if $f \leq C \cdot g$ (or $f \geq C \cdot g$) for some constant $C > 0$ when r is large enough. $f(r) = \Theta(g(r))$ if both $f(r) = \mathcal{O}(g(r))$ and $f(r) = \Omega(g(r))$ holds, where $c \cdot g \leq f \leq C \cdot g$ for some constant $0 \leq c \leq C$ when r is large enough.

2 PROBLEM FORMULATION

Given N pairs of training samples $\mathcal{D} = \{\boldsymbol{x}_n, y_n\}_{n=1}^N$ where $\boldsymbol{x}_n \in \mathbb{R}^d$ represent input features and $y_n \in \mathbb{R}$ represents the corresponding output label, the learning problem is to find the model weights of the given architecture of neural networks such that the learned model has the minimum testing error on the testing data drawn from the same distribution as the training data. Here we consider the setup of model estimation and assume that for any input $\boldsymbol{x}$, the resulting output y is generated by a sparse one-hidden-layer neural network, as shown in Fig. 1.

Specifically, we consider a weight-sparse neural network with K neurons where each neuron is connected to r[1] ($r \leq d$) input features. Note that $r \ll d$ for a sparse network. Let $\boldsymbol{W}^* \in \mathbb{R}^{r \times K}$ contain all the ground truth weights of the K neurons, where the j-th column, denoted by $\boldsymbol{w}_j^* \in \mathbb{R}^r$, contains the edge weights connected to the j-th neuron. Let Ω_j denote the set of indices of the input features to which the j-th neuron is connected. Given input $\boldsymbol{x}_n$, let $\boldsymbol{x}_{n,\Omega_j} \in \mathbb{R}^r$ represent the sub-vector that is connected to j-th neuron, where $j \in [K]$. Then, in a regression problem, y_n is obtained by [2]

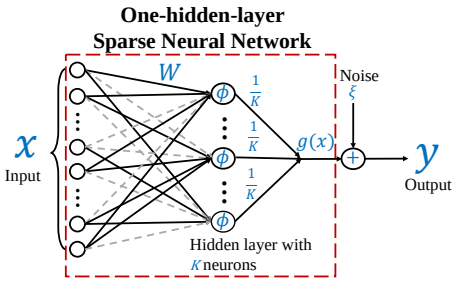

Figure 1: Illustration of the model

$$y_n = \frac{1}{K} \sum_{j=1}^{K} \phi(\boldsymbol{w}_j^{*T} \boldsymbol{x}_{n,\Omega_j}) + \xi_n := g(\boldsymbol{x}_n; \boldsymbol{W}^*) + \xi_n, \quad (1)$$

where ξ_n is the unknown additive noise and ϕ is the activation function.

Following the standard assumption in (Zhong et al., 2017), $\boldsymbol{x}_n$ is independent and identically distributed (i.i.d.) from the standard Gaussian distribution $\mathcal{N}(\boldsymbol{0}, \boldsymbol{I}_{d \times d})$. Throughout the paper, we consider rectified linear unit (ReLU), where $\phi(z) = \max\{z, 0\}$. ξ_n can be arbitrary, and we only assume ξ_n is bounded as $|\xi_n| \leq |\xi|$ for some constant ξ. Given any estimated $\boldsymbol{W} = [\boldsymbol{w}_1, \boldsymbol{w}_2, \cdots, \boldsymbol{w}_K] \in \mathbb{R}^{r \times K}$ of the weight matrix $\boldsymbol{W}^*$, the empirical risk function with respect to the training set $\mathcal{D}$ is

$$\hat{f}_{\mathcal{D}}(\boldsymbol{W}) = \frac{1}{2N} \sum_{n=1}^{N} \Big(\frac{1}{K} \sum_{j=1}^{K} \phi(\boldsymbol{w}_j^T \boldsymbol{x}_{n,\Omega_j}) - y_n \Big)^2, \quad (2)$$

[1] We consider the same r for each neuron in this paper, but the analysis can be easily modified to handle the case of different numbers of features per neuron.

[2] The analysis is extendable to binary classification, and the output is generated by $\text{Prob}\big(y_n = 1 | \boldsymbol{x}_n\big) = g(\boldsymbol{x}_n; \boldsymbol{W}^*)$.

where we consider the square loss function here. The learning objective is to estimate the ground-truth weight matrix $\boldsymbol{W}^*$ from the training samples $\mathcal{D}$ via solving the following problem:

$$\min_{\boldsymbol{W}\in\mathbb{R}^{r\times K}} \quad \hat{f}_{\mathcal{D}}(\boldsymbol{W}). \tag{3}$$

Clearly, $\boldsymbol{W}^*$ is a global minimizer to (3) when measurements are noiseless, i.e., $\xi_n = 0$ for all n. The questions that this paper addresses include: (1) **what algorithm** to estimate the ground-truth model? (2) what is the **sample complexity** for the accurate estimate? (3) what is the **impact of the network pruning** on the difficulty of the learning problem and the performance of the learned model?

Connections with dense networks. To connect with conventional dense neural networks, we define an augmented matrix $\widetilde{\boldsymbol{W}}^* \in \mathbb{R}^{d\times K}$, where the j-th column of $\widetilde{\boldsymbol{W}}^*$, denoted by $\widetilde{\boldsymbol{w}}_j^*$, contains the weights connected to the j-th neuron, and $\widetilde{\boldsymbol{W}}^*$ is zero padded in other entries for non-existing weights. In other words, $\widetilde{\boldsymbol{w}}_{j,\Omega_j}^* = \boldsymbol{w}_j^*$ for all $j \in [K]$, and $\widetilde{W}_{ij}^* = 0$ if $i \notin \Omega_j$. The mask matrix $\boldsymbol{M}$, as discussed in (Frankle & Carbin, 2019), with respect to $\boldsymbol{W}^*$ is defined as $M_{ij} = 1$ if $i \in \Omega_j$, and $M_{ij} = 0$ otherwise. Then, we have $\boldsymbol{M} \odot \widetilde{\boldsymbol{W}}^* = \widetilde{\boldsymbol{W}}^*$, where $\odot$ stands for the entry-wise multiplication. In (Frankle & Carbin, 2019), an Iterative Magnitude Pruning (IMP) algorithm is proposed to compute the mask matrix $\boldsymbol{M}$ for the lottery ticket. In this paper, we assume the binary mask $\boldsymbol{M}$ is known *a priori* (namely, it can be accurately found). Equation (3) can be equivalently written as

$$\min_{\widetilde{\boldsymbol{W}}\in\mathbb{R}^{d\times K}} \hat{f}_{\mathcal{D}}(\widetilde{\boldsymbol{W}}) = \frac{1}{2N}\sum_{n=1}^{N}\Big(\frac{1}{K}\sum_{j=1}^{K}\phi(\widetilde{\boldsymbol{w}}_j^T\boldsymbol{x}_n) - y_n\Big)^2, \qquad \text{s.t. } \widetilde{\boldsymbol{W}} = \boldsymbol{M}\odot\widetilde{\boldsymbol{W}}, \tag{4}$$

where $\widetilde{\boldsymbol{W}} = [\widetilde{\boldsymbol{w}}_1, \widetilde{\boldsymbol{w}}_2, \cdots, \widetilde{\boldsymbol{w}}_K] \in \mathbb{R}^{d\times K}$ is an estimate of the augmented weight matrix $\widetilde{\boldsymbol{W}}^*$. $\widetilde{\boldsymbol{W}}^*$ is a global minimizer to (4) when measurements are noiseless. Note that (4) differs from the learning problem of the conventional dense networks in the additional constraint $\boldsymbol{M}\odot\widetilde{\boldsymbol{W}} = \widetilde{\boldsymbol{W}}$. When $\boldsymbol{M}$ is an all-one matrix, i.e., $r = d$, (4) reduces to the conventional learning problem of an one-hidden-layer neural network.

3 Local Geometric Structure

We defer the algorithmic design and analysis to Section 4 and study the geometric structure of (2) here. Theorem 1 characterizes the local convexity of $\hat{f}_{\mathcal{D}}(\boldsymbol{W})$ in (2). It has two important implications.

1. **Strictly local convex ball around $\boldsymbol{W}^*$**: $\hat{f}_{\mathcal{D}}(\boldsymbol{W})$ is strictly convex around $\boldsymbol{W}^*$, and the radius of the convex ball is negatively correlated with $\sqrt{r}$, where r is the number of non-pruned weights per neuron. Thus, the convex ball enlarges as r decreases.

2. **Importance of the winning ticket architecture**: Compared with training on the dense network directly, training on a correctly pruned sub-network has a larger convex region near $\boldsymbol{W}^*$, which may lead to easier estimation of $\boldsymbol{W}^*$. To some extend, this result can be viewed as a theoretical validation of the importance of the winning architecture (a good sub-network) in (Frankle & Carbin, 2019). Formally, we have

Theorem 1 (Local Convexity)**.** *Suppose constants ε_0, $\varepsilon_1 \in (0,1)$. When the number of samples satisfies*

$$N = \Omega\big(\varepsilon_1^{-2}K^4 r\log d\big), \tag{5}$$

then for any $\boldsymbol{W}$ that satisfies

$$\|\boldsymbol{W} - \boldsymbol{W}^*\|_F = \mathcal{O}\Big(\frac{\varepsilon_0}{K^2}\Big), \tag{6}$$

we have

$$\Theta\Big(\frac{1-\varepsilon_0-\varepsilon_1}{K^2}\Big)\boldsymbol{I} \preceq \nabla^2\hat{f}_{\mathcal{D}}(\boldsymbol{W}) \preceq \Theta\Big(\frac{1}{K}\Big)\boldsymbol{I}. \tag{7}$$

Theorem 1 shows that with enough samples as shown in (5), in a local region of $\boldsymbol{W}^*$ as shown in (6), all the eigenvalues of Hessian matrix of the empirical risk function are lower and upper bounded by two positive constants. This property is useful in designing efficient algorithms to recover $\boldsymbol{W}^*$, as shown in Section 4.

Moreover, when the number of samples N is fixed and r changes, ε_1 can be $\Theta(\sqrt{r})$ while (5) is still met. ε_0 in (7) can be arbitrarily close to but small than $1-\varepsilon_1$ so that the Hessian matrix is still positive definite. Then from (6), the radius of the convex ball is $\Theta(1) - \Theta(\sqrt{r})$, indicating an enlarged region when r decreases.

4 Convergence Analysis with Accelerated Gradient Descent

We propose to solve the non-convex problem (3) via the accelerated gradient descent (AGD) algorithm, summarized in Algorithm 1. Compared with the vanilla gradient descent (GD) algorithm, AGD has an additional momentum term, denoted by $\beta(\boldsymbol{W}^{(t)} - \boldsymbol{W}^{(t-1)})$, in each iteration. AGD enjoys a faster convergence rate than GD in solving optimization problems including learning neural networks (Zhang et al., 2020b). GD can be viewed as a special case of AGD by letting $\beta = 0$.

The initial point $\boldsymbol{W}^{(0)}$ can be obtained through a tensor initialization method, which is built upon Algorithm 1 in (Zhong et al., 2017) for fully connected neural networks with modification to handle a sparse neural network. Specifically, we reduce the complexity dependence from input data dimension d to the sparsity r, the definitions of the high-order moments (see (11)-(13) in Appendix A) are modified by replacing $\boldsymbol{x}$ in Definition 5.1 in Zhong et al. (2017) with $\tilde{\boldsymbol{x}} = \frac{1}{\sqrt{K}} \sum_{j=1}^{K} \boldsymbol{x}_{\Omega_j} \in \mathbb{R}^r$. Details of the tensor initialization method are provided in Appendix A.

Algorithm 1 Accelerated Gradient Descent (AGD) Algorithm

1: **Input:** training data $\mathcal{D} = \{(\boldsymbol{x}_n, y_n)\}_{n=1}^N$, gradient step size η, momentum parameter β, and an initialization $\boldsymbol{W}^{(0)}$ by the tensor initialization method;
2: Partition $\mathcal{D}$ into $T = \log(1/\varepsilon)$ disjoint subsets, denoted as $\{\mathcal{D}_t\}_{t=1}^T$;
3: **for** $t = 1, 2, \cdots, T$ **do**
4: $\quad \boldsymbol{W}^{(t+1)} = \boldsymbol{W}^{(t)} - \eta \nabla_{\boldsymbol{W}} \hat{f}_{\mathcal{D}_t}(\boldsymbol{W}^{(t)}) + \beta(\boldsymbol{W}^{(t)} - \boldsymbol{W}^{(t-1)})$
5: **end for**
6: **Return:** $\boldsymbol{W}^{(T)}$

The theoretical analyses of our algorithm are summarized in Theorem 2 (convergence) and Lemma 1 (Initialization). The significance of these results can be interpreted from the following aspects.

1. **Linear convergence to the ground-truth model**: Theorem 2 implies that if initialized in the local convex region, the iterates generated by AGD converge linearly to the ground truth $\boldsymbol{W}^*$ when noiseless. When there is noise, they converge to a point $\boldsymbol{W}^{(T)}$. The distance between $\boldsymbol{W}^{(T)}$ and $\boldsymbol{W}^*$ is proportional to the noise level and scales in terms of $\mathcal{O}(\sqrt{r/N})$. Moreover, when N is fixed, the convergence rate of AGD is $\Theta(\sqrt{r/K})$, while the rate is $\Theta(\sqrt{r}/K)$ for the vanilla GD algorithm, indicating faster convergence of AGD. Lemma 1 shows the tensor initialization method indeed returns an initial point in the convex region.

2. **Sample complexity for accurate estimate**: We show that the required number of samples for successful estimation is $\Theta(r \log d)$, which is order-wise optimal with respect to the number of non-pruned neuron weights r, and only logarithmic with respect to the input feature dimension d. Our sample complexity is much less than the conventional bound of $\Theta(d \log d)$ for one-hidden-layer networks (Zhong et al., 2017; Zhang et al., 2020a;c). This is the first theoretical characterization of learning a pruned network from the perspective of sample complexity.

3. **Improved generalization of winning tickets**: We prove that with a fixed number of training samples, training on a properly pruned sub-network converges faster to $\boldsymbol{W}^*$ than training on the original dense network. Our theoretical analysis justifies that training on the winning ticket can meet or exceed the same test accuracy within the same number of iterations. To the best of our knowledge, our result here provides the first theoretical justification for this intriguing empirical finding of "improved generalization of winning tickets" by (Frankle & Carbin, 2019).

Theorem 2 (Convergence)**.** *Suppose $\boldsymbol{W}^{(0)}$ satisfies* (6) *and the number of samples satisfies*

$$N = \Omega\big(\varepsilon_0^{-2} K^8 r \log d \log(1/\varepsilon)\big) \tag{8}$$

for some $\varepsilon_0 \in (0, 1/2)$. Let $\eta = K/14$ in Algorithm 1. Then the iterates $\{\boldsymbol{W}^{(t)}\}_{t=1}^T$ returned by Algorithm 1 converges linearly to $\boldsymbol{W}^*$ up to the noise level with probability at least $1 - K^2 T \cdot d^{-10}$ as

$$\begin{aligned} \|\boldsymbol{W}^{(t)} - \boldsymbol{W}^*\|_F &\le \nu(\beta)^t \|\boldsymbol{W}^{(0)} - \boldsymbol{W}^*\|_F + \mathcal{O}\left(\sqrt{\frac{K^2 r \log d}{N}}\right) \cdot |\xi|, \\ \text{and} \quad \|\boldsymbol{W}^{(T)} - \boldsymbol{W}^*\|_F &\le \varepsilon \|\boldsymbol{W}^*\|_F + \mathcal{O}\left(\sqrt{\frac{K^2 r \log d}{N}}\right) \cdot |\xi| \end{aligned} \tag{9}$$

where $\nu(\beta)$ is the rate of convergence that depends on β with $\nu(\beta^*) = 1 - \Theta\big(\frac{1-\varepsilon_0}{\sqrt{K}}\big)$ for some non-zero β^* and $\nu(0) = 1 - \Theta\big(\frac{1-\varepsilon_0}{K}\big)$.

Lemma 1 (Initialization)**.** *Assume the noise $|\xi| \le \|\boldsymbol{W}^*\|_2$ and the number of samples $N = \Omega\big(\varepsilon_0^{-2} K^8 r \log^4 d\big)$ for $\varepsilon_0 > 0$, the tensor initialization method outputs $\boldsymbol{W}^{(0)}$ such that (6) holds, i.e., $\|\boldsymbol{W}^{(0)} - \boldsymbol{W}^*\|_F = \mathcal{O}\big(\frac{\varepsilon_0 \sigma_K}{K^2}\big)$.*

With a fixed number of samples, when r decreases, ε_0 can be $\Theta(\sqrt{r})$ while the condition in (8) is still met. Then $\nu(0) = \Theta(\sqrt{r}/K)$ and $\nu(\beta^*) = \Theta(\sqrt{r/K})$. Therefore, when r decreases, both the stochastic and accelerated gradient descent converge faster. The theoretical bound of the improvement of the convergence rate by accelerated gradient descent is the same as that in (Zhang et al., 2020a;c). However, (Zhang et al., 2020a;c) focus on convolutional neural networks without any network pruning, while our results consider pruned networks. Note that as long as $\boldsymbol{W}^{(0)}$ is initialized in the local convex region, not necessarily by the tensor method, Theorem 2 guarantees the accurate recovery.

5 Numerical Experiments

We first verify our theoretical results on synthetic data and then analyze the pruning performance of the IMP algorithm (Frankle & Carbin, 2019) on both synthetic data and real data. The synthetic data are generated using a ground-truth sparse neural network in Fig. 1. The input $\{\boldsymbol{x}_n\}_{n=1}^N$ are randomly generated from Gaussian distribution $\mathcal{N}(0, \boldsymbol{I}_{d\times d})$ independently, and the index set $\Omega_j (1 \le j \le K)$ is generated by selecting r numbers randomly from $[d]$ without replacement. Each entry of the weight matrix $\boldsymbol{W}^*$ is randomly selected from $[-0.5, 0.5]$ independently. The noise $\{\xi_n\}_{n=1}^N$ are i.i.d. from $\mathcal{N}(0, \sigma^2)$, and the noise level is measured by σ/E_y, where E_y is the average energy of the noiseless outputs $\{g(\boldsymbol{x}_n; \boldsymbol{W}^*)\}_{n=1}^N$ calculated as $E_y = \sqrt{\frac{1}{N}\sum_{n=1}^N |g(\boldsymbol{x}_n; \boldsymbol{W}^*)|^2}$.

Algorithm 1 is implemented with two minor modifications. First, the initial point is randomly selected from $\big\{\boldsymbol{W}^{(0)} \big| \|\boldsymbol{W}^{(0)} - \boldsymbol{W}^*\|_F / \|\boldsymbol{W}^*\|_F < \lambda\big\}$ for some constant $\lambda > 0$ to reduce the computation. Second, we use the whole training data instead of a fresh subset in each iteration. Algorithm 1 terminates when $\|\boldsymbol{W}^{(t+1)} - \boldsymbol{W}^{(t)}\|_F / \|\boldsymbol{W}^{(t)}\|_F$ is smaller than 10^{-8} or reaching 10000 number of iterations. In Section 5.2,

we implement the IMP algorithm (Frankle & Carbin, 2019) [3] to prune the neural network. The real dataset we use is the MNIST dataset, and the network architecture is Lenet-5 structure (Lecun et al., 1998).

5.1 EVALUATION OF THEORETICAL FINDINGS ON SYNTHETIC DATA

Local convexity near the ground-truth. We set the number of neurons $K = 5$, the dimension of the data $d = 500$ and the sample size $N = 3000$. Figure 2 illustrates the success rate of Algorithm 1 when the network sparsity changes. The y-axis is the relative distance of the initialization $\boldsymbol{W}^{(0)}$ to the ground-truth. For each pair of r and the initial distance, we run 100 independent tests, and the network weights, training data and the initialization $\boldsymbol{W}^{(0)}$ are all generated independently in each test. Each test is called successful if the relative error of the solution $\boldsymbol{W}$ returned by Algorithm 1, measured by $\|\boldsymbol{W} - \boldsymbol{W}^*\|_2/\|\boldsymbol{W}^*\|_2$, is less than 10^{-4}. A black block means Algorithm 1 fails in estimating $\boldsymbol{W}^*$ in all runs while a white block indicates all successes. Algorithm 1 succeeds if $\boldsymbol{W}^{(0)}$ is in the local convex region near $\boldsymbol{W}^*$. From Figure 2, we can see that the radius of convex region is indeed linear in $-\sqrt{r}$, as predicted by Theorem 1.

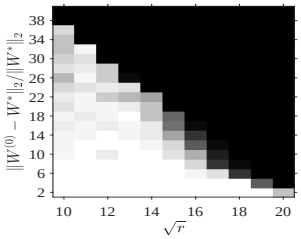

Figure 2: The radius of the local convex region against $\sqrt{r}$

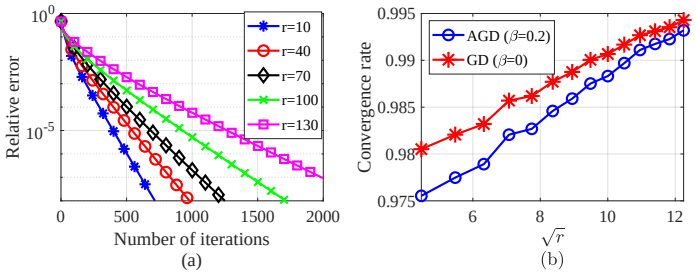

Figure 3: Convergence rate when r changes

Convergence rate. Figure 3 shows the convergence rate of Algorithm 1 when r changes. $N = 3000$, $d = 300$, $K = 5$, $\eta = 0.5$, and $\beta = 0.2$. Figure 3(a) shows that the relative error decreases exponentially as the number of iterations increases, indicating the linear convergence of Algorithm 1. As shown in Figure 3(b), the convergence rate is almost linear in $\sqrt{r}$, as predicted by Theorem 2. We also compare with GD by setting β as 0. One can see that AGD has a smaller convergence rate than GD, indicating faster convergence.

Sample complexity. Figure 4 shows the phrase transition of Algorithm 1 when varying N and r. d is fixed as 100. For each value of N, we construct 100 independent runs where the ground-truth model and training data are generated independently in each run. We can see that the required number of samples for successful estimation is linear in r, as predicted by (8).

Performance in noisy case. Figure 5 shows the relative error of the learned model by Algorithm 1 from noisy measurements when r changes. $N = 1000$, $K = 10$, and $d = 300$. The relative error is linear in $\sqrt{r}$, as predicted by (9). Moreover, the relative error is proportional to the noise level $|\xi|$.

5.2 IMP FOR FINDING WINNING TICKETS

Here we implement the IMP algorithm to obtain pruned networks on both synthetic data and real data. Figure 6 shows the test performance of a pruned network on synthetic data with different sample sizes. Here in the ground-truth network model, $K = 5, d = 100$, and $r/d = 20\%$. The noise level $\sigma/E_y = 10^{-3}$. One observation is that for a fixed sample size N greater than 100, the test error decreases as the number of remaining parameters decreases. This verifies that the IMP algorithm indeed prunes the network properly. It also shows that the learned model improves as the pruning progresses, verifying our theoretical result in

[3] The code is downloaded from https://github.com/rahulvigneswaran/Lottery-Ticket-Hypothesis-in-Pytorch.

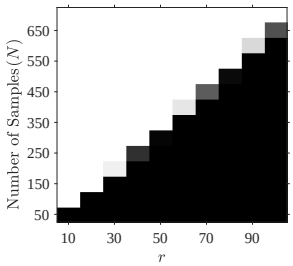

Figure 4: Sample complexity when r changes

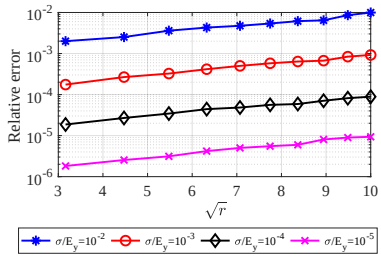

Figure 5: Relative error against $\sqrt{r}$ at different noise level

Theorem 2 that the difference of the learned model from the ground-truth model decreases as the number of remaining weights decreases. The second observation is that the test error decreases as N increases for any fixed number of remaining parameters. This verifies our result in Theorem 2 that the difference of the learned model from the ground-truth model decreases as the number of training samples increases. When the network is pruned significantly such that the percentage of reaming parameters is less than the ground-truth 20%, the pruned network cannot explain the data properly, and thus the test error is large for all N. When the number of samples is too small, $N = 100$, the test error is always large, because it does not meet the sample complexity requirement for estimating the sparse model even though the network is properly pruned.

Figure 7 shows the performance of the IMP algorithm on MNIST dataset using Lenet5 architecture. The percentage of weights to be pruned after each cycle is 20%, and other parameters are set as default values. Although not as obvious as the results on synthetic data, we still observe the same phenomenon of the performance when pruning progresses. That is, the test accuracy first increases when we properly prune the network (e.g., the case of $N = 20000$), indicating the effectiveness of proper pruning. By contrast, the test accuracy drops as the network is overly pruned.

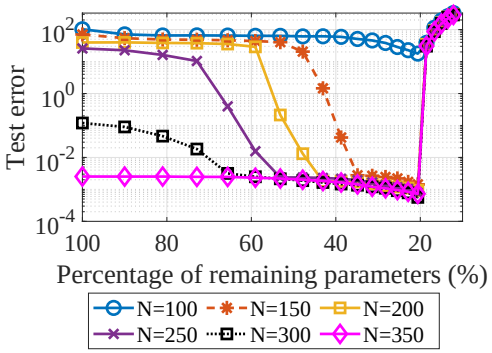

Figure 6: Test error of pruned models on the synthetic dataset

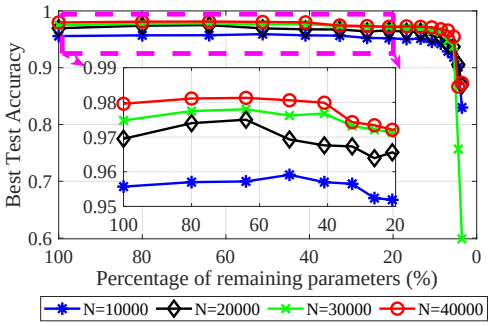

Figure 7: Test accuracy of pruned models on MNIST dataset

6 Conclusions

This paper provides the first theoretical analysis of learning one-hidden-layer sparse neural networks, which offers formal justification of the improved generalization of winning ticket observed from empirical findings in LTH. We characterize analytically the impact of the number of remaining weights in a pruned network on the required number of samples for training, the convergence rate of learning algorithm, and the accuracy of the learned model. We also provide extensive numerical validations of our theoretical findings. One desired future work will be generalizing our theoretical analysis to the scenario of network pruning on multi-layer neural networks.

REFERENCES

Sanjeev Arora, Rong Ge, Behnam Neyshabur, and Yi Zhang. Stronger generalization bounds for deep nets via a compression approach. In Jennifer Dy and Andreas Krause (eds.), *Proceedings of the 35th International Conference on Machine Learning*, volume 80 of *Proceedings of Machine Learning Research*, pp. 254–263, StockholmsmÃssan, Stockholm Sweden, 10–15 Jul 2018. PMLR. URL http://proceedings.mlr.press/v80/arora18b.html.

Rajendra Bhatia. *Matrix analysis*, volume 169. Springer Science & Business Media, 2013.

Alon Brutzkus and Amir Globerson. Globally optimal gradient descent for a convnet with gaussian inputs. In *Proceedings of the 34th International Conference on Machine Learning-Volume 70*, pp. 605–614. JMLR. org, 2017.

Tianlong Chen, Jonathan Frankle, Shiyu Chang, Sijia Liu, Yang Zhang, Zhangyang Wang, and Michael Carbin. The lottery ticket hypothesis for pre-trained bert networks. *arXiv preprint arXiv:2007.12223*, 2020a.

Tianlong Chen, Jonathan Frankle, Shiyu Chang, Sijia Liu, Yang Zhang, Zhangyang Wang, and Michael Carbin. The lottery ticket hypothesis for pre-trained bert networks. *arXiv preprint arXiv:2007.12223*, 2020b.

Xin Dong, Shangyu Chen, and Sinno Pan. Learning to prune deep neural networks via layer-wise optimal brain surgeon. In *Advances in Neural Information Processing Systems*, pp. 4857–4867, 2017.

Simon S Du, Jason D Lee, Yuandong Tian, Aarti Singh, and Barnabas Poczos. Gradient descent learns one-hidden-layer cnn: Don't be afraid of spurious local minima. In *International Conference on Machine Learning*, pp. 1338–1347, 2018.

Utku Evci, Trevor Gale, Jacob Menick, Pablo Samuel Castro, and Erich Elsen. Rigging the lottery: Making all tickets winners. *International Conference on Machine Learning*, 2020.

Jonathan Frankle and Michael Carbin. The lottery ticket hypothesis: Finding sparse, trainable neural networks. In *International Conference on Learning Representations*, 2019. URL https://openreview.net/forum?id=rJl-b3RcF7.

Jonathan Frankle, Gintare Karolina Dziugaite, Daniel M Roy, and Michael Carbin. Stabilizing the lottery ticket hypothesis. *arXiv preprint arXiv:1903.01611*, 2019a.

Jonathan Frankle, Gintare Karolina Dziugaite, Daniel M Roy, and Michael Carbin. Linear mode connectivity and the lottery ticket hypothesis. *arXiv preprint arXiv:1912.05671*, 2019b.

Haoyu Fu, Yuejie Chi, and Yingbin Liang. Guaranteed recovery of one-hidden-layer neural networks via cross entropy. *arXiv preprint arXiv:1802.06463*, 2018.

Song Han, Jeff Pool, John Tran, and William Dally. Learning both weights and connections for efficient neural network. In *Advances in neural information processing systems*, pp. 1135–1143, 2015.

Babak Hassibi and David G Stork. Second order derivatives for network pruning: Optimal brain surgeon. In *Advances in neural information processing systems*, pp. 164–171, 1993.

Hengyuan Hu, Rui Peng, Yu-Wing Tai, and Chi-Keung Tang. Network trimming: A data-driven neuron pruning approach towards efficient deep architectures. *arXiv preprint arXiv:1607.03250*, 2016.

Volodymyr Kuleshov, Arun Chaganty, and Percy Liang. Tensor factorization via matrix factorization. In *Artificial Intelligence and Statistics*, pp. 507–516, 2015.

Y. Lecun, L. Bottou, Y. Bengio, and P. Haffner. Gradient-based learning applied to document recognition. *Proceedings of the IEEE*, 86(11):2278–2324, 1998.

Yann LeCun, John S Denker, and Sara A Solla. Optimal brain damage. In *Advances in neural information processing systems*, pp. 598–605, 1990.

Zhuang Liu, Mingjie Sun, Tinghui Zhou, Gao Huang, and Trevor Darrell. Rethinking the value of network pruning. In *International Conference on Learning Representations*, 2018.

Roi Livni, Shai Shalev-Shwartz, and Ohad Shamir. On the computational efficiency of training neural networks. In *Advances in neural information processing systems*, pp. 855–863, 2014.

Eran Malach, Gilad Yehudai, Shai Shalev-Shwartz, and Ohad Shamir. Proving the lottery ticket hypothesis: Pruning is all you need. *arXiv preprint arXiv:2002.00585*, 2020.

Dmitry Molchanov, Arsenii Ashukha, and Dmitry Vetrov. Variational dropout sparsifies deep neural networks. In *International Conference on Machine Learning*, pp. 2498–2507, 2017.

Vivek Ramanujan, Mitchell Wortsman, Aniruddha Kembhavi, Ali Farhadi, and Mohammad Rastegari. What's hidden in a randomly weighted neural network? In *Proceedings of the IEEE/CVF Conference on Computer Vision and Pattern Recognition*, pp. 11893–11902, 2020.

Alex Renda, Jonathan Frankle, and Michael Carbin. Comparing rewinding and fine-tuning in neural network pruning. In *International Conference on Learning Representations*, 2019.

Itay Safran and Ohad Shamir. Spurious local minima are common in two-layer relu neural networks. In *International Conference on Machine Learning*, pp. 4430–4438, 2018.

Ohad Shamir. Distribution-specific hardness of learning neural networks. *The Journal of Machine Learning Research*, 19(1):1135–1163, 2018.

Mahdi Soltanolkotabi, Adel Javanmard, and Jason D Lee. Theoretical insights into the optimization landscape of over-parameterized shallow neural networks. *IEEE Transactions on Information Theory*, 65(2): 742–769, 2018.

Suraj Srinivas and R Venkatesh Babu. Data-free parameter pruning for deep neural networks. *arXiv preprint arXiv:1507.06149*, 2015.

Yuandong Tian. An analytical formula of population gradient for two-layered relu network and its applications in convergence and critical point analysis. In *Proceedings of the 34th International Conference on Machine Learning-Volume 70*, pp. 3404–3413. JMLR. org, 2017.

Joel A Tropp. User-friendly tail bounds for sums of random matrices. *Foundations of computational mathematics*, 12(4):389–434, 2012.

Roman Vershynin. Introduction to the non-asymptotic analysis of random matrices. *arXiv preprint arXiv:1011.3027*, 2010.

Chaoqi Wang, Guodong Zhang, and Roger Grosse. Picking winning tickets before training by preserving gradient flow. In *International Conference on Learning Representations*, 2019.

Tien-Ju Yang, Yu-Hsin Chen, and Vivienne Sze. Designing energy-efficient convolutional neural networks using energy-aware pruning. In *Proceedings of the IEEE Conference on Computer Vision and Pattern Recognition*, pp. 5687–5695, 2017.

Gilad Yehudai and Ohad Shamir. On the power and limitations of random features for understanding neural networks. In *Advances in Neural Information Processing Systems*, pp. 6594–6604, 2019.

Haoran You, Chaojian Li, Pengfei Xu, Yonggan Fu, Yue Wang, Xiaohan Chen, Richard G Baraniuk, Zhangyang Wang, and Yingyan Lin. Drawing early-bird tickets: Toward more efficient training of deep networks. In *International Conference on Learning Representations*, 2019.

Chiyuan Zhang, Samy Bengio, Moritz Hardt, Benjamin Recht, and Oriol Vinyals. Understanding deep learning requires rethinking generalization. *arXiv preprint arXiv:1611.03530*, 2016.

Shuai Zhang, Meng Wang, Sijia Liu, Pin-Yu Chen, and Jinjun Xiong. Guaranteed convergence of training convolutional neural networks via accelerated gradient descent. In *2020 54th Annual Conference on Information Sciences and Systems (CISS)*, 2020a. URL doi:10.1109/CISS48834.2020.1570627111.

Shuai Zhang, Meng Wang, Sijia Liu, Pin-Yu Chen, and Jinjun Xiong. Fast learning of graph neural networks with guaranteed generalizability:one-hidden-layer case. In *2020 International Conference on Machine Learning (ICML)*, 2020b.

Shuai Zhang, Meng Wang, Sijia Liu, Pin-Yu Chen, and Jinjun Xiong. Learning one-hidden-layer convolutional neural networks via accelerated gradient descent with generalizability guarantees. *submitted to IEEE Transactions on Neural Networks and Learning Systems*, 2020c.

Kai Zhong, Zhao Song, Prateek Jain, Peter L Bartlett, and Inderjit S Dhillon. Recovery guarantees for one-hidden-layer neural networks. In *Proceedings of the 34th International Conference on Machine Learning-Volume 70*, pp. 4140–4149. JMLR. org, https://arxiv.org/abs/1706.03175, 2017.

Hattie Zhou, Janice Lan, Rosanne Liu, and Jason Yosinski. Deconstructing lottery tickets: Zeros, signs, and the supermask. In *Advances in Neural Information Processing Systems 32*, pp. 3597–3607. 2019.

Wenda Zhou, Victor Veitch, Morgane Austern, Ryan P Adams, and Peter Orbanz. Non-vacuous generalization bounds at the imagenet scale: a pac-bayesian compression approach. In *International Conference on Learning Representations*, 2018.

A INITIALIZATION VIA TENSOR METHOD

Following Zhong et al. (2017), we define a special outer product, denoted by $\widetilde{\otimes}$. For any vector $\boldsymbol{v} \in \mathbb{R}^{d_1}$ and $\boldsymbol{Z} \in \mathbb{R}^{d_1 \times d_2}$,

$$\boldsymbol{v} \widetilde{\otimes} \boldsymbol{Z} = \sum_{i=1}^{d_2} (\boldsymbol{v} \otimes \boldsymbol{z}_i \otimes \boldsymbol{z}_i + \boldsymbol{z}_i \otimes \boldsymbol{v} \otimes \boldsymbol{z}_i + \boldsymbol{z}_i \otimes \boldsymbol{z}_i \otimes \boldsymbol{v}), \tag{10}$$

where $\otimes$ is the outer product and $\boldsymbol{z}_i$ is the i-th column of $\boldsymbol{Z}$. Recall that $\widetilde{\boldsymbol{x}} = \frac{1}{\sqrt{K}} \sum_{j=1}^{K} \boldsymbol{x}_{\Omega_j}$ Next, we define the high order momentum in the following way:

$$\boldsymbol{M}_1 = \mathbb{E}_{\boldsymbol{x}}\{y \tilde{\boldsymbol{x}}\} \in \mathbb{R}^d, \tag{11}$$

$$\boldsymbol{M}_2 = \mathbb{E}_{\boldsymbol{x}}\Big[y\big(\tilde{\boldsymbol{x}} \otimes \tilde{\boldsymbol{x}} - \mathbb{E}_{\boldsymbol{x}} \tilde{\boldsymbol{x}} \tilde{\boldsymbol{x}}^T\big)\Big] \in \mathbb{R}^{d \times d}, \tag{12}$$

$$\boldsymbol{M}_3 = \mathbb{E}_{\boldsymbol{x}}\Big[y\big(\tilde{\boldsymbol{x}}^{\otimes 3} - \widetilde{\boldsymbol{x}} \widetilde{\otimes} \mathbb{E}_{\boldsymbol{x}} \widetilde{\boldsymbol{x}} \widetilde{\boldsymbol{x}}^T\big)\Big] \in \mathbb{R}^{d \times d \times d}, \tag{13}$$

where $\boldsymbol{z}^{\otimes 3} := \boldsymbol{z} \otimes \boldsymbol{z} \otimes \boldsymbol{z}$, and $\mathbb{E}_{\boldsymbol{x}}$ is the expectation over $\boldsymbol{x}$.

Following the same calculate formulas in the Claim 5.2 (Zhong et al., 2017), there exist some known constants $\psi_i, i = 1, 2, 3$, such that

$$\boldsymbol{M}_1 = \sum_{j=1}^{K} \psi_1 \cdot \|\boldsymbol{w}_j^*\|_2 \cdot \overline{\boldsymbol{w}}_j^*, \tag{14}$$

$$\boldsymbol{M}_2 = \sum_{j=1}^{K} \psi_2 \cdot \|\boldsymbol{w}_j^*\|_2 \cdot \overline{\boldsymbol{w}}_j^* \overline{\boldsymbol{w}}_j^{*T}, \tag{15}$$

$$\boldsymbol{M}_3 = \sum_{j=1}^{K} \psi_3 \cdot \|\boldsymbol{w}_j^*\|_2 \cdot \overline{\boldsymbol{w}}_j^{*\otimes 3}, \tag{16}$$

where $\overline{\boldsymbol{w}}_j^* = \boldsymbol{w}_j^* / \|\boldsymbol{w}_j^*\|_2$ in (11)-(13) is the normalization of $\boldsymbol{w}_j^*$.

$\boldsymbol{M}_1$, $\boldsymbol{M}_2$ and $\boldsymbol{M}_3$ can be estimated through the samples $\big\{(\boldsymbol{x}_n, y_n)\big\}_{n=1}^N$, and let $\widehat{\boldsymbol{M}}_1$, $\widehat{\boldsymbol{M}}_2$, $\widehat{\boldsymbol{M}}_3$ denote the corresponding estimates. First, we will decompose the rank-k tensor $\boldsymbol{M}_3$ and obtain the $\{\overline{\boldsymbol{w}}_j^*\}_{j=1}^K$. By applying the tensor decomposition method Kuleshov et al. (2015) to $\widehat{\boldsymbol{M}}_3$, the outputs, denoted by $\widehat{\overline{\boldsymbol{w}}}_j^*$, are the estimations of $\{\overline{\boldsymbol{w}}_j^*\}_{j=1}^K$. Next, we will estimate $\|\boldsymbol{w}_j^*\|_2$ through solving the following optimization problem:

$$\widehat{\boldsymbol{\alpha}} = \arg\min_{\boldsymbol{\alpha} \in \mathbb{R}^K} : \quad \Big|\widehat{\boldsymbol{M}}_1 - \sum_{j=1}^{K} \psi_1 \alpha_j \widehat{\overline{\boldsymbol{w}}}_j^*\Big|, \tag{17}$$

From (14) and (17), we know that $|\widehat{\alpha}_j|$ is the estimation of $\|\boldsymbol{w}_j^*\|_2$. Thus, $\boldsymbol{W}^{(0)}$ is given as $\big[\widehat{\alpha}_1 \widehat{\overline{\boldsymbol{w}}}_1^*, \cdots, \widehat{\alpha}_j \widehat{\overline{\boldsymbol{w}}}_j^*, \cdots, \widehat{\alpha}_K \widehat{\overline{\boldsymbol{w}}}_K^*\big]$.

To reduce the computational complexity of tensor decomposition, one can project $\widehat{\boldsymbol{M}}_3$ to a lower-dimensional tensor (Zhong et al., 2017). The idea is to first estimate the subspace spanned by $\{\boldsymbol{w}_j^*\}_{j=1}^K$, and let $\widehat{\boldsymbol{V}}$ denote the estimated subspace.

Moreover, we have

$$\boldsymbol{M}_3(\widehat{\boldsymbol{V}}, \widehat{\boldsymbol{V}}, \widehat{\boldsymbol{V}}) = \mathbb{E}_{\boldsymbol{x}}\Big[y\big((\widehat{\boldsymbol{V}}^T \widetilde{\boldsymbol{x}})^{\otimes 3} - (\widehat{\boldsymbol{V}}^T \widetilde{\boldsymbol{x}}) \widetilde{\otimes} \mathbb{E}_{\boldsymbol{x}} (\widehat{\boldsymbol{V}}^T \widetilde{\boldsymbol{x}})(\widehat{\boldsymbol{V}}^T \widetilde{\boldsymbol{x}})^T\big)\Big] \in \mathbb{R}^{K \times K \times K}, \tag{18}$$

Subroutine 1 Tensor Initialization Method

1: **Input:** training data $\mathcal{D} = \{(\boldsymbol{x}_n, y_n)\}_{n=1}^N$;
2: Partition $\mathcal{D}$ into three disjoint subsets $\mathcal{D}_1$, $\mathcal{D}_2$, $\mathcal{D}_3$;
3: Calculate $\widehat{\boldsymbol{M}}_1$, $\widehat{\boldsymbol{M}}_2$ following (11), (12) using $\mathcal{D}_1$, $\mathcal{D}_2$, respectively;
4: Obtain the estimate subspace $\widehat{\boldsymbol{V}}$ of $\widehat{\boldsymbol{M}}_2$;
5: Calculate $\widehat{\boldsymbol{M}}_3(\widehat{\boldsymbol{V}}, \widehat{\boldsymbol{V}}, \widehat{\boldsymbol{V}})$ through $\mathcal{D}_3$;
6: Obtain $\{\widehat{\boldsymbol{u}}_j\}_{j=1}^K$ via tensor decomposition method Kuleshov et al. (2015);
7: Obtain $\widehat{\boldsymbol{\alpha}}$ by solving optimization problem (17);
8: **Return:** $\boldsymbol{w}_j^{(0)} = \widehat{\alpha}_j \widehat{\boldsymbol{V}} \widehat{\boldsymbol{u}}_j$, $j = 1, ..., K$.

Then, one can decompose the estimate $\widehat{\boldsymbol{M}}_3(\widehat{\boldsymbol{V}}, \widehat{\boldsymbol{V}}, \widehat{\boldsymbol{V}})$ to obtain unit vectors $\{\widehat{\boldsymbol{u}}_j\}_{j=1}^K \in \mathbb{R}^K$. Since $\overline{\boldsymbol{w}}^*$ lies in the subspace $\boldsymbol{V}$, we have $\boldsymbol{V}\boldsymbol{V}^T\overline{\boldsymbol{w}}_j^* = \overline{\boldsymbol{w}}_j^*$. Then, $\widehat{\boldsymbol{V}}\widehat{\boldsymbol{u}}_j$ is an estimate of $\overline{\boldsymbol{w}}_j^*$. The initialization process is summarized in Subroutine 1.

B NOTATIONS

In this section, we summarize some important notations that will be used in the following proofs. First, recall that the empirical risk function over data $\mathcal{D} = \{(\boldsymbol{x}_n, y_n)\}_{n=1}^N$ in (2) is defined as

$$\hat{f}_{\mathcal{D}}(\boldsymbol{W}) = \frac{1}{2N} \sum_{n=1}^N \Big(\frac{1}{K} \sum_{j=1}^K \phi(\boldsymbol{w}_j^T \boldsymbol{x}_{n,\Omega_j}) - y_n \Big)^2. \tag{19}$$

In addition, the population risk function, which is the expectation of the empirical risk function over the data $\mathcal{D}$, is defined as

$$\begin{aligned} f(\boldsymbol{W}) = \mathbb{E}_{\mathcal{D}} \hat{f}_{\mathcal{D}}(\boldsymbol{W}) =& \mathbb{E}_{\mathcal{D}} \frac{1}{2N} \sum_{n=1}^N \Big(\frac{1}{K} \sum_{j=1}^K \phi(\boldsymbol{w}_j^T \boldsymbol{x}_{n,\Omega_j}) - y_n \Big)^2 \\ =& \mathbb{E}_{\boldsymbol{x}} \frac{1}{2} \Big(\frac{1}{K} \sum_{j=1}^K \phi(\boldsymbol{w}_j^T \boldsymbol{x}_{\Omega_j}) - y \Big)^2, \end{aligned} \tag{20}$$

where $\boldsymbol{x} \in \mathbb{R}^d$ belongs to standard Gaussian distribution, and $y = g(\boldsymbol{W}^*; \boldsymbol{x})$. Besides these, we use σ_i to denote the i-th largest singular value of $\boldsymbol{W}^*$. Then, κ is defined as σ_1/σ_K, and $\gamma = \prod_{i=1}^K \sigma_i/\sigma_K$. ρ is defined in Property 3.2 (Zhong et al., 2017) and a fixed constant for the ReLU activation function.

Next, to avoid high dimensional tensor in analyzing the second order derivative of the objective function. The proofs will be based on $\text{Vec}(\boldsymbol{W}) \in \mathbb{R}^{Kr}$, which is the vectorized $\boldsymbol{W}$, instead. For notational convenience, we will still use $\boldsymbol{W}$ in the proofs, but $\boldsymbol{W}$ is a vector instead of a matrix. Hence, the first order derivative of the empirical risk function $\nabla \hat{f}_{\mathcal{D}} \in \mathbb{R}^{Kr}$, and the second order derivative $\nabla^2 \hat{f}_{\mathcal{D}} \in \mathbb{R}^{Kr \times Kr}$.

Moreover, without special descriptions, $\boldsymbol{\alpha} = [\boldsymbol{\alpha}_1^T, \boldsymbol{\alpha}_2^T, \cdots, \boldsymbol{\alpha}_K^T]^T$ stands for any unit vectors that in $\mathbb{R}^{Kr}$ with $\boldsymbol{\alpha}_j \in \mathbb{R}^r$. Therefore, we have

$$\|\nabla^2 \hat{f}_{\mathcal{D}}\|_2 = \max_{\boldsymbol{\alpha}} \|\boldsymbol{\alpha}^T \nabla^2 \hat{f}_{\mathcal{D}} \boldsymbol{\alpha}\|_2 = \max_{\boldsymbol{\alpha}} \Big(\sum_{j=1}^K \boldsymbol{\alpha}_j^T \frac{\partial \hat{f}_{\mathcal{D}}}{\partial \boldsymbol{w}_j} \Big)^2. \tag{21}$$

Finally, since we focus on order-wise analysis, some constant number will be ignored in majority of the steps. In particular, we use $h_1(z) \gtrsim$ (or $\lesssim, \eqsim$)$h_2(z)$ to denote there exists some positive constant C such that $h_1(z) \geq$ (or $\leq, =$)$C \cdot h_2(z)$ when z is sufficiently large.

C Proof of Theorem 1

The main idea in proving Theorem 1 is to use triangle inequality as shown in (25) by bounding the second order derivative of the population risk function and the distance between the empirical risk and population risk functions. Lemma 3 provides the lower and upper bound for the population risk function, while Lemma 4 provides the error bound between the second order derivation of empirical risk and population risk functions.

Lemma 2 (Weyl's inequality, Bhatia (2013))**.** *Suppose $\boldsymbol{B} = \boldsymbol{A} + \boldsymbol{E}$ be a matrix with dimension $m \times m$. Let $\lambda_i(\boldsymbol{B})$ and $\lambda_i(\boldsymbol{A})$ be the i-th largest eigenvalues of $\boldsymbol{B}$ and $\boldsymbol{A}$, respectively. Then, we have*

$$|\lambda_i(\boldsymbol{B}) - \lambda_i(\boldsymbol{A})| \leq \|\boldsymbol{E}\|_2, \quad \forall i \in [m]. \tag{22}$$

Lemma 3. *Let f be the population risk function in* (20)*. Assume $\boldsymbol{W}$ satisfies* (6)*, then the second-order derivative of f over $\boldsymbol{W}$ is bounded as*

$$\frac{(1-\varepsilon_0)\rho}{11\kappa^2\gamma K^2}\boldsymbol{I} \leq \nabla^2 f(\boldsymbol{W}) \leq \frac{7}{K}\boldsymbol{I}. \tag{23}$$

Lemma 4. *Let $\hat{f}_{\mathcal{D}}$ and f be the empirical and population risk function in* (19) *and* (20)*, respectively, then the second-order derivative of $\hat{f}_{\mathcal{D}}$ is colse to its expectation f with an upper bound as:*

$$\|\nabla^2 \hat{f}_{\mathcal{D}} - \nabla^2 f\|_2 \lesssim \sqrt{\frac{r \log d}{N}}. \tag{24}$$

Proof of Theorem 1 . Let $\hat{\lambda}_{\max}$ and $\hat{\lambda}_{\min}$ denote the largest and smallest eigenvalues of $\nabla^2 \hat{f}_{\mathcal{D}}$, respectively. Also, Let $\lambda_{\max}$ and $\lambda_{\min}$ denote the largest and smallest eigenvalues of $\nabla^2 f_{\mathcal{D}}$, respectively.

Then, from Lemma 2, we have

$$\hat{\lambda}_{\max} \leq \lambda_{\max} + \|\nabla^2 \hat{f}_{\mathcal{D}} - \nabla^2 f\|_2 \tag{25}$$

and

$$\hat{\lambda}_{\min} \geq \lambda_{\min} - \|\nabla^2 \hat{f}_{\mathcal{D}} - \nabla^2 f\|_2. \tag{26}$$

When the sample complexity satisfies $N \gtrsim \varepsilon_1^{-2}\rho^{-2}\kappa^4\gamma^2 K^4 r \log d$, then from Lemma 4, we have

$$\|\nabla^2 \hat{f}_{\mathcal{D}} - \nabla^2 f\|_2 \leq \frac{\varepsilon_1 \rho}{11\kappa^2\gamma K^2}. \tag{27}$$

Then, from (25), (26) and (27), we have

$$\hat{\lambda}_{\max} \leq \frac{8}{K}, \tag{28}$$

and

$$\hat{\lambda}_{\min} \geq \frac{(1-\varepsilon_0-\varepsilon_1)\rho}{11\kappa^2\gamma K^2}, \tag{29}$$

which completes the proof. □

D PROOF OF THEOREM 2

The major idea in proving Theorem 2 is to first characterize the gradient descent term as

$$\begin{aligned}\nabla \hat{f}_{\Omega_t}(\boldsymbol{W}^{(t)}) =& f_{\Omega_t}(\boldsymbol{W}^{(t)}) + \big(\hat{f}_{\Omega_t}(\boldsymbol{W}^{(t)}) - f_{\Omega_t}(\boldsymbol{W}^{(t)})\big) \\ =& \langle \nabla^2 f_{\Omega_t}(\widehat{\boldsymbol{W}}^{(t)}), \boldsymbol{W}^{(t)} - \boldsymbol{W}^*\rangle + \big(\hat{f}_{\Omega_t}(\boldsymbol{W}^{(t)}) - f_{\Omega_t}(\boldsymbol{W}^{(t)})\big),\end{aligned} \tag{30}$$

where the last inequality is obtained through intermediate value theorem, and $\widehat{\boldsymbol{W}}^{(t)}$ lies in the convex hull of $\boldsymbol{W}^{(t)}$ and $\boldsymbol{W}^*$. The reason that intermediate value theorem is applied on population risk function instead of empirical risk function is the non-smoothness of the empirical risk functions. Due to the non-smoothness of ReLU activation function at zero point, the empirical risk function is not smooth, either. However, the expectation of the empirical risk function over the Gaussian input $\boldsymbol{x}$ is smooth. Hence, compared with smooth empirical risk function, i.e., neural networks equipped with sigmoid activation function, we have an additional lemma to bound $\nabla \hat{f}_{\mathcal{D}_t}$ to its expectation ∇f , which is summarized in Lemma 5.

The momentum term $\beta(\boldsymbol{W}^{(t)} - \boldsymbol{W}^{(t-1)})$ plays an important role in determining the convergence rate, and the recursive rule is obtained in the following way:

$$\begin{bmatrix}\boldsymbol{W}^{(t+1)} - \boldsymbol{W}^* \\ \boldsymbol{W}^{(t)} - \boldsymbol{W}^*\end{bmatrix} = \boldsymbol{A}(\beta)\begin{bmatrix}\boldsymbol{W}^{(t)} - \boldsymbol{W}^* \\ \boldsymbol{W}^{(t-1)} - \boldsymbol{W}^*\end{bmatrix}, \tag{31}$$

where $\boldsymbol{A}(\beta)$ is a matrix with respect to the value of β and defined in (36). Then, we know iterates $\boldsymbol{W}^{(t)}$ converge to the ground-truth with a linear rate which is the largest singlar value of matrix $\boldsymbol{A}(\beta)$. Recall that AGD reduces to GD with $\beta = 0$, so our analysis applies to GD method as well. We are able to show the convergence rate of AGD is faster than GD by proving the largest singluar value of $\boldsymbol{A}(\beta)$ is smaller than $\boldsymbol{A}(0)$ for some $\beta > 0$.

Lemma 5. *Let $\hat{f}_{\mathcal{D}}$ and f be the empirical and population risk function in* (19) *and* (20)*, respectively, then the first-order derivative of $\hat{f}_{\mathcal{D}}$ is close to its expectation f with an upper bound as:*

$$\|\nabla \hat{f}_{\mathcal{D}}(\boldsymbol{W}) - \nabla f(\boldsymbol{W})\|_2 \lesssim \sqrt{\frac{r\log d}{N}}\big(\|\boldsymbol{W} - \boldsymbol{W}^*\|_2 + \xi\big). \tag{32}$$

Proof of Theorem 2. The update rule of $\boldsymbol{W}^{(t)}$ is

$$\begin{aligned}\boldsymbol{W}^{(t+1)} =& \boldsymbol{W}^{(t)} - \eta\nabla \hat{f}_{\mathcal{D}_t}(\boldsymbol{W}^{(t)}) + \beta(\boldsymbol{W}^{(t)} - \boldsymbol{W}^{(t-1)}) \\ =& \boldsymbol{W}^{(t)} - \eta\nabla f(\boldsymbol{W}^{(t)}) + \beta(\boldsymbol{W}^{(t)} - \boldsymbol{W}^{(t-1)}) + \eta(\nabla f(\boldsymbol{W}^{(t)}) - \nabla \hat{f}_{\mathcal{D}_t}(\boldsymbol{W}^{(t)}))\end{aligned} \tag{33}$$

Since $\nabla^2 f$ is a smooth function, by the intermediate value theorem, we have

$$\begin{aligned}\boldsymbol{W}^{(t+1)} = \boldsymbol{W}^{(t)} - \eta\nabla^2 f(\widehat{\boldsymbol{W}}^{(t)})(\boldsymbol{W}^{(t)} - \boldsymbol{W}^*) + \beta(\boldsymbol{W}^{(t)} - \boldsymbol{W}^{(t-1)}) \\ + \eta\big(\nabla f(\boldsymbol{W}^{(t)}) - \nabla \hat{f}_{\mathcal{D}_t}(\boldsymbol{W}^{(t)})\big),\end{aligned} \tag{34}$$

where $\widehat{\boldsymbol{W}}^{(t)}$ lies in the convex hull of $\boldsymbol{W}^{(t)}$ and $\boldsymbol{W}^*$.
Next, we have

$$\begin{aligned}\begin{bmatrix}\boldsymbol{W}^{(t+1)} - \boldsymbol{W}^* \\ \boldsymbol{W}^{(t)} - \boldsymbol{W}^*\end{bmatrix} = \begin{bmatrix}\boldsymbol{I} - \eta\nabla^2 f(\widehat{\boldsymbol{W}}^{(t)}) + \beta\boldsymbol{I} & \beta\boldsymbol{I} \\ \boldsymbol{I} & 0\end{bmatrix}\begin{bmatrix}\boldsymbol{W}^{(t)} - \boldsymbol{W}^* \\ \boldsymbol{W}^{(t-1)} - \boldsymbol{W}^*\end{bmatrix} \\ + \eta\begin{bmatrix}\nabla f(\boldsymbol{W}^{(t)}) - \nabla \hat{f}_{\mathcal{D}_t}(\boldsymbol{W}^{(t)}) \\ 0\end{bmatrix}\end{aligned} \tag{35}$$

Let

$$\boldsymbol{A}(\beta) = \begin{bmatrix} \boldsymbol{I} - \eta\nabla^2 f(\widehat{\boldsymbol{W}}^{(t)}) + \beta\boldsymbol{I} & \beta\boldsymbol{I} \\ \boldsymbol{I} & 0 \end{bmatrix}, \tag{36}$$

so we have

$$\left\| \begin{bmatrix} \boldsymbol{W}^{(t+1)} - \boldsymbol{W}^* \\ \boldsymbol{W}^{(t)} - \boldsymbol{W}^* \end{bmatrix} \right\|_2 = \|\boldsymbol{A}(\beta)\|_2 \left\| \begin{bmatrix} \boldsymbol{W}^{(t)} - \boldsymbol{W}^* \\ \boldsymbol{W}^{(t-1)} - \boldsymbol{W}^* \end{bmatrix} \right\|_2 + \eta \left\| \begin{bmatrix} \nabla f(\boldsymbol{W}^{(t)}) - \nabla \hat{f}_{\mathcal{D}_t}(\boldsymbol{W}^{(t)}) \\ 0 \end{bmatrix} \right\|_2.$$

From Lemma 5, we know that

$$\eta \left\| \nabla f(\boldsymbol{W}^{(t)}) - \nabla \hat{f}_{\mathcal{D}_t}(\boldsymbol{W}^{(t)}) \right\|_2 \leq C_5 \eta \sqrt{\frac{r\log d}{N_t}} \Big(\|\boldsymbol{W} - \boldsymbol{W}^*\|_2 + |\xi| \Big) \tag{37}$$

for some constant $C_5 > 0$. Then, we have

$$\begin{aligned} \|\boldsymbol{W}^{(t+1)} - \boldsymbol{W}^*\|_2 \leq & \left(\|\boldsymbol{A}(\beta)\|_2 + C_5\eta\sqrt{\frac{r\log d}{N_t}} \right) \|\boldsymbol{W}^{(t)} - \boldsymbol{W}^*\|_2 + C_5\eta\sqrt{\frac{r\log d}{N_t}}|\xi| \\ := & \nu(\beta)\|\boldsymbol{W}^{(t)} - \boldsymbol{W}^*\|_2 + C_5\eta\sqrt{\frac{r\log d}{N_t}}|\xi|. \end{aligned} \tag{38}$$

Let $\nabla^2 f(\widehat{\boldsymbol{W}}^{(t)}) = \boldsymbol{S}\boldsymbol{\Lambda}\boldsymbol{S}^T$ be the eigendecomposition of $\nabla^2 f(\widehat{\boldsymbol{W}}^{(t)})$. Then, we define

$$\boldsymbol{A}(\beta) := \begin{bmatrix} \boldsymbol{S}^T & \boldsymbol{0} \\ \boldsymbol{0} & \boldsymbol{S}^T \end{bmatrix} \boldsymbol{A}(\beta) \begin{bmatrix} \boldsymbol{S} & \boldsymbol{0} \\ \boldsymbol{0} & \boldsymbol{S} \end{bmatrix} = \begin{bmatrix} \boldsymbol{I} - \eta\boldsymbol{\Lambda} + \beta\mathbf{I} & \beta\boldsymbol{I} \\ \boldsymbol{I} & 0 \end{bmatrix} \tag{39}$$

Since $\begin{bmatrix} \boldsymbol{S} & \boldsymbol{0} \\ \boldsymbol{0} & \boldsymbol{S} \end{bmatrix} \begin{bmatrix} \boldsymbol{S}^T & \boldsymbol{0} \\ \boldsymbol{0} & \boldsymbol{S}^T \end{bmatrix} = \begin{bmatrix} \boldsymbol{I} & \boldsymbol{0} \\ \boldsymbol{0} & \boldsymbol{I} \end{bmatrix}$, we know $\boldsymbol{A}(\beta)$ and $\boldsymbol{A}(\beta)$ share the same eigenvalues.

Let λ_i be the i-th eigenvalue of $\nabla^2 f(\widehat{\boldsymbol{W}}^{(t)})$, then the corresponding i-th eigenvalue of (39), denoted by $\delta_i(\beta)$, satisfies

$$\nu_i^2 - (1 - \eta\lambda_i + \beta)\delta_i + \beta = 0. \tag{40}$$

Then, we have

$$\delta_i(\beta) = \frac{(1 - \eta\lambda_i + \beta) + \sqrt{(1 - \eta\lambda_i + \beta)^2 - 4\beta}}{2}, \tag{41}$$

and

$$|\delta_i(\beta)| = \begin{cases} \sqrt{\beta}, & \text{if} \quad \beta \geq \big(1 - \sqrt{\eta\lambda_i}\big)^2, \\ \frac{1}{2}\left| (1 - \eta\lambda_i + \beta) + \sqrt{(1 - \eta\lambda_i + \beta)^2 - 4\beta} \right|, & \text{otherwise.} \end{cases} \tag{42}$$

Note that the other root of (40) is abandoned because the root in (41) is always larger than or at least equal to the other root with $|1 - \eta\lambda_i| < 1$. By simple calculation, we have

$$\delta_i(0) > \delta_i(\beta), \quad \text{for} \quad \forall \beta \in \big(0, (1 - \eta\lambda_i)^2\big), \tag{43}$$

and specifically, δ_i achieves the minimum $\delta_i^* = |1 - \sqrt{\eta\lambda_i}|$ when $\beta = \big(1 - \sqrt{\eta\lambda_i}\big)^2$.

Let us first assume $\boldsymbol{W}^{(t)}$ satisfies (6), then from Lemma 3, we know that

$$0 < \frac{(1 - \varepsilon_0)}{11\kappa^2\gamma K^2} \leq \lambda_i \leq \frac{7}{K}.$$

Let $\gamma_1 = \frac{\rho(1-\varepsilon_0)}{11\kappa^2\gamma K^2}$ and $\gamma_2 = \frac{7}{K}$. If we choose β such that

$$\beta^* = \max\big\{(1 - \sqrt{\eta\gamma_1})^2, (1 - \sqrt{\eta\gamma_2})^2\big\}, \tag{44}$$

then we have $\beta \geq (1-\sqrt{\eta\lambda_i})^2$ for any i and $\delta_i = \max\left\{|1-\sqrt{\eta\gamma_1}|, |1-\sqrt{\eta\gamma_2}|\right\}$ for any i.

Let $\eta = \frac{1}{2\gamma_2}$, then β^* equals to $\left(1-\sqrt{\frac{\gamma_1}{2\gamma_2}}\right)^2$. Then, for any $\varepsilon_0 \in (0, \frac{1}{2})$ we have

$$\begin{aligned}\|\boldsymbol{A}(\beta^*)\|_2 = \max_i \delta_i(\beta^*) = 1-\sqrt{\frac{\gamma_1}{2\gamma_2}} =& 1-\sqrt{\frac{1-\varepsilon_0}{154\rho^{-1}\kappa^2\gamma K}} \\ \leq& 1-\frac{1-3/4\cdot\varepsilon_0}{\sqrt{154\rho^{-1}\kappa^2\gamma K}}.\end{aligned} \tag{45}$$

Then, let

$$C_5\eta\sqrt{\frac{r\log d}{N_t}} \leq \frac{\varepsilon_0}{4\sqrt{154\rho^{-1}\kappa^2\gamma K}}, \tag{46}$$

we need $N_t \gtrsim \varepsilon_0^{-2}\rho^{-1}\kappa^2\gamma K^3 r\log d$.

Combine (45) and (46), we have

$$\nu(\beta^*) \leq 1-\frac{1-\varepsilon_0}{\sqrt{154\rho^{-1}\kappa^2\gamma K}}. \tag{47}$$

While let $\beta = 0$, we have

$$\nu(0) \geq \|\boldsymbol{A}(0)\|_2 = 1-\frac{1-\varepsilon_0}{154\rho^{-1}\kappa^2\gamma K} \tag{48}$$

and

$$\nu(0) \leq \|\boldsymbol{A}(0)\|_2 + C_5\eta\sqrt{\frac{r\log d}{N_t}} \leq 1-\frac{1-2\varepsilon_0}{154\rho^{-1}\kappa^2\gamma K} \tag{49}$$

if $N_t \gtrsim \varepsilon_0^{-2}\rho^{-1}\kappa^2\gamma K^4 r\log d$.

In conclusion, with $\eta = \frac{1}{2\gamma_2}$ and $\beta = \left(1-\frac{\gamma_1}{2\gamma_2}\right)^2$, we have

$$\|\boldsymbol{W}^{(t+1)} - \boldsymbol{W}^*\|_2 \leq \left(1-\frac{1-\varepsilon_0}{\sqrt{154\kappa^2\gamma K}}\right)\|\boldsymbol{W}^{(t)} - \boldsymbol{W}^*\|_2 + 2C\eta\sqrt{\frac{r\log d}{N_t}}|\xi|. \tag{50}$$

if $\boldsymbol{W}^{(t+1)}$ satisfies (6) and $N_t \gtrsim \varepsilon_0^{-2}\kappa^2\gamma K^3 r\log d$.

Then, we can start mathematical induction of (50) over t.

Base case: (6) holds for $\boldsymbol{W}^{(0)}$ naturally from the assumption in Theorem 2. Since (6) holds and the number of samples exceeds the required bound in (50), we have (50) holds for $t = 0$.

Induction step: Assume (50) holds for t, to make sure the mathematical induction of (50) holds, we need $\boldsymbol{W}^{(t+1)}$ satisfies (6). That is

$$\eta\sqrt{\frac{d\log d}{N_t}} \lesssim \frac{1-\varepsilon_0}{\sqrt{132\kappa^2\gamma K}}\cdot\frac{\varepsilon_0\sigma_K}{44\kappa^2\gamma K^2}. \tag{51}$$

Hence, we need

$$N_t \gtrsim \varepsilon_0^{-2}\kappa^8\gamma^3 K^6 d\log d. \tag{52}$$

In conclusion, when $N_t \gtrsim \varepsilon_0^{-2}\kappa^9\gamma^3 K^8 d\log^4 d$, we know that (50) holds for all $1 \leq t \leq T$ with probability at least $1 - K^2T\cdot d^{-10}$. By simple calculation, we can obtain

$$\|\boldsymbol{W}^{(T)} - \boldsymbol{W}^*\|_2 \leq \left(1-\frac{1-\varepsilon_0}{\sqrt{132\kappa^2\gamma K}}\right)^T\|\boldsymbol{W}^{(0)} - \boldsymbol{W}^*\|_2 + C\sqrt{\frac{\kappa^2\gamma K^2 r\log d}{N_t}}\cdot|\xi|. \tag{53}$$

for some constant $C > 0$.

□

E PROOF OF LEMMA 1

Instead of providing the proof for Lemma 1, we turn to prove a more general bound for the performance of tensor initialization method as shown in Lemma 6. One easily verify that Lemma 1 holds naturally from Lemma 6.

Lemma 6. *Assume the noise level $|\xi| \leq K\sigma_1$ and the number of samples $N \gtrsim \kappa^8 K^8 r \log^6 d$, the tensor initialization method in Subroutine 1 outputs $\boldsymbol{W}^{(0)}$ such that*

$$\|\boldsymbol{W}^{(0)} - \boldsymbol{W}^*\|_2 \lesssim \kappa^6 \sqrt{\frac{K^4 r \log d}{N}}(\sigma_1 + |\xi|) \tag{54}$$

with probability at least $1 - d^{-10}$.

E.1 PROOF OF LEMMA 6

Lemma 7. *Suppose $\boldsymbol{M}_2$ is defined as in* (12) *and $\widehat{\boldsymbol{M}}_2$ is the estimation of $\boldsymbol{M}_2$ by samples $\mathcal{D} = \{(\boldsymbol{x}_n, y_n)\}_{n=1}^N$. Then, with probability $1 - d^{-10}$, we have*

$$\|\widehat{\boldsymbol{M}}_2 - \boldsymbol{M}_2\| \lesssim \sqrt{\frac{r \log d}{N}}(\sigma_1 + |\xi|), \tag{55}$$

provided that $N \gtrsim r \log^4 d$.

Lemma 8. *Let $\widehat{\boldsymbol{V}}$ be generated by step 4 in Subroutine 1. Suppose $\boldsymbol{M}_3(\widehat{\boldsymbol{V}}, \widehat{\boldsymbol{V}}, \widehat{\boldsymbol{V}})$ is defined as in* (18) *and $\widehat{\boldsymbol{M}}_3(\widehat{\boldsymbol{V}}, \widehat{\boldsymbol{V}}, \widehat{\boldsymbol{V}})$ is the estimation of $\boldsymbol{M}_3(\widehat{\boldsymbol{V}}, \widehat{\boldsymbol{V}}, \widehat{\boldsymbol{V}})$ by samples $\mathcal{D} = \{(\boldsymbol{x}_n, y_n)\}_{n=1}^N$. Further, we assume $\boldsymbol{V} \in \mathbb{R}^{r \times K}$ is an orthogonal basis of $\boldsymbol{W}^*$ and satisfies $\|\boldsymbol{V}\boldsymbol{V}^T - \widehat{\boldsymbol{V}}\widehat{\boldsymbol{V}}^T\| \leq 1/4$. Then, provided that $N \gtrsim K^5 \log^6 d$, with probability at least $1 - d^{-10}$, we have*

$$\|\widehat{\boldsymbol{M}}_3(\widehat{\boldsymbol{V}}, \widehat{\boldsymbol{V}}, \widehat{\boldsymbol{V}}) - \boldsymbol{M}_3(\widehat{\boldsymbol{V}}, \widehat{\boldsymbol{V}}, \widehat{\boldsymbol{V}})\| \lesssim \sqrt{\frac{K^3 \log d}{N}}(\sigma_1 + |\xi|). \tag{56}$$

Lemma 9. *Suppose $\boldsymbol{M}_1$ is defined as in* (11) *and $\widehat{\boldsymbol{M}}_1$ is the estimation of $\boldsymbol{M}_1$ by samples $\mathcal{D} = \{(\boldsymbol{x}_n, y_n)\}_{n=1}^N$. Then, with probability $1 - d^{-10}$, we have*

$$\|\widehat{\boldsymbol{M}}_1 - \boldsymbol{M}_1\| \lesssim \sqrt{\frac{r \log d}{N}}(\sigma_1 + |\xi|) \tag{57}$$

provided that $N \gtrsim r \log^4 d$.

Lemma 10 (Tropp (2012), Theorem 1.6)**.** *Consider a finite sequence $\{\boldsymbol{Z}_k\}$ of independent, random matrices with dimensions $d_1 \times d_2$. Assume that such random matrix satisfies*

$$\mathbb{E}(\boldsymbol{Z}_k) = 0 \quad \textit{and} \quad \|\boldsymbol{Z}_k\| \leq R \quad \textit{almost surely}.$$

Define

$$\delta^2 := \max\Big\{\Big\|\sum_k \mathbb{E}(\boldsymbol{Z}_k \boldsymbol{Z}_k^*)\Big\|, \Big\|\sum_k \mathbb{E}(\boldsymbol{Z}_k^* \boldsymbol{Z}_k)\Big\|\Big\}.$$

Then for all $t \geq 0$, we have

$$\textit{Prob}\Big\{\Big\|\sum_k \boldsymbol{Z}_k\Big\| \geq t\Big\} \leq (d_1 + d_2)\exp\Big(\frac{-t^2/2}{\delta^2 + Rt/3}\Big).$$

Lemma 11 (Zhong et al. (2017), Lemma E.6)**.** *Let $\boldsymbol{V} \in \mathbb{R}^{r\times K}$ be an orthogonal basis of $\boldsymbol{W}^*$ and $\widehat{\boldsymbol{V}}$ be generated by step 4 in Subroutine 1. Assume $\|\widehat{\boldsymbol{M}}_2 - \boldsymbol{M}_2\|_2 \le \sigma_K(\boldsymbol{M}_2)/10$. Then, we have*

$$\|\boldsymbol{V}\boldsymbol{V}^T - \widehat{\boldsymbol{V}}\widehat{\boldsymbol{V}}^T\|_2 \le \frac{\|\boldsymbol{M}_2 - \widehat{\boldsymbol{M}}_2\|}{\sigma_K(\boldsymbol{M}_2)}. \tag{58}$$

Lemma 12 (Zhong et al. (2017), Lemmas E.13 and E.14)**.** *Let $\boldsymbol{V} \in \mathbb{R}^{r\times K}$ be an orthogonal basis of $\boldsymbol{W}^*$ and $\widehat{\boldsymbol{V}}$ be generated by step 4 in Subroutine 1. Assume $\boldsymbol{M}_1$ can be written in the form of* (14) *with some constant ψ_1, and let $\widehat{\boldsymbol{M}}_1$ be the estimation of $\boldsymbol{M}_1$ by samples $\mathcal{D} = \{\boldsymbol{x}_n, y_n\}_{n=1}^N$. Let $\widehat{\boldsymbol{\alpha}}$ be the optimal solutions of* (17) *with $\widehat{\overline{\boldsymbol{w}}}_j = \widehat{\boldsymbol{V}}\widehat{\boldsymbol{u}}_j$. Then, for each $j \in \{1, 2, \cdots, K\}$, if*

$$\begin{aligned} T_1 &:= \|\boldsymbol{V}\boldsymbol{V}^T - \widehat{\boldsymbol{V}}\widehat{\boldsymbol{V}}^T\|_2 \le \frac{1}{\kappa^2\sqrt{K}}, \\ T_2 &:= \|\widehat{\boldsymbol{u}}_j - \widehat{\boldsymbol{V}}^T\overline{\boldsymbol{w}}_j\|_2 \le \frac{1}{\kappa^2\sqrt{K}}, \\ T_3 &:= \|\widehat{\boldsymbol{M}}_1 - \boldsymbol{M}_1\|_2 \le \frac{1}{4}\|\boldsymbol{M}_1\|_2, \end{aligned} \tag{59}$$

then we have

$$\left|\alpha_j^* - \widehat{\alpha}_j\right| \le \left(\kappa^4 K^{\frac{3}{2}}\big(T_1 + T_2\big) + \kappa^2 K^{\frac{1}{2}} T_3\right)|\alpha_j^*|, \tag{60}$$

where $\alpha_j^* = \|\boldsymbol{w}_j^*\|_2$.

Proof of Lemma 1. By simple calculation, we have

$$\begin{aligned} &\|\boldsymbol{w}_j^* - |\widehat{\alpha}_j|\widehat{\boldsymbol{V}}\widehat{\boldsymbol{u}}_j\|_2 \\ \le&\left\|\boldsymbol{w}_j^* - \|\boldsymbol{w}_j\|_2\widehat{\boldsymbol{V}}\widehat{\boldsymbol{u}}_j + \|\boldsymbol{w}_j\|_2\widehat{\boldsymbol{V}}\widehat{\boldsymbol{u}}_j - |\widehat{\alpha}_j|\widehat{\boldsymbol{V}}\widehat{\boldsymbol{u}}_j\right\|_2 \\ \le&\left\|\boldsymbol{w}_j^* - \|\boldsymbol{w}_j\|_2\widehat{\boldsymbol{V}}\widehat{\boldsymbol{u}}_j\right\|_2 + \left\|\|\boldsymbol{w}_j\|_2\widehat{\boldsymbol{V}}\widehat{\boldsymbol{u}}_j - |\widehat{\alpha}_j|\widehat{\boldsymbol{V}}\widehat{\boldsymbol{u}}_j\right\|_2 \\ \le&\|\boldsymbol{w}_j^*\|_2\|\overline{\boldsymbol{w}}_j^* - \widehat{\boldsymbol{V}}\widehat{\boldsymbol{u}}_j\|_2 + \left|\|\boldsymbol{w}_j\|_2 - |\widehat{\alpha}_j|\right|\|\widehat{\boldsymbol{V}}\widehat{\boldsymbol{u}}_j\|_2 \\ \le&\sigma_1\big(\|\overline{\boldsymbol{w}}_j^* - \widehat{\boldsymbol{V}}\widehat{\boldsymbol{V}}^T\overline{\boldsymbol{w}}_j^*\|_2 + \|\widehat{\boldsymbol{V}}^T\overline{\boldsymbol{w}}_j^* - \widehat{\boldsymbol{u}}_j\|_2\big) + \left|\|\boldsymbol{w}_j\|_2 - |\widehat{\alpha}_j|\right| \\ :=&\sigma_1\big(I_1 + I_2\big) + I_3. \end{aligned} \tag{61}$$

From Lemma 11, we have

$$I_1 = \|\overline{\boldsymbol{w}}_j^* - \widehat{\boldsymbol{V}}\widehat{\boldsymbol{V}}^T\overline{\boldsymbol{w}}_j^*\|_2 \le \|\boldsymbol{V}\boldsymbol{V}^T - \widehat{\boldsymbol{V}}\widehat{\boldsymbol{V}}^T\|_2 \le \frac{\|\widehat{\boldsymbol{M}}_2 - \boldsymbol{M}_2\|_2}{\sigma_K(\boldsymbol{M}_2)}, \tag{62}$$

where the last inequality comes from Lemma 7. Then, from (15), we know that

$$\sigma_K(\boldsymbol{M}_2) \lesssim \min_{1\le j\le K}\|\boldsymbol{w}_j\|_2 \lesssim \sigma_K. \tag{63}$$

From Theorem 3 in (Kuleshov et al., 2015), we have

$$I_2 = \|\widehat{\boldsymbol{V}}^T\overline{\boldsymbol{w}}_j^* - \widehat{\boldsymbol{u}}_j\|_2 \lesssim \frac{\kappa}{\sigma_K}\|\widehat{\boldsymbol{M}}_3(\widehat{\boldsymbol{V}}, \widehat{\boldsymbol{V}}, \widehat{\boldsymbol{V}}) - \boldsymbol{M}_3(\widehat{\boldsymbol{V}}, \widehat{\boldsymbol{V}}, \widehat{\boldsymbol{V}})\|_2. \tag{64}$$

To guarantee the condition (59) in Lemma 12 hold, according to Lemmas 7 and 8, we need $N \gtrsim \kappa^3 K r \log d$. Then, from Lemma 12, we have

$$I_3 = \left(\kappa^4 K^{3/2}(I_1 + I_2) + \kappa^2 K^{1/2}\|\widehat{\boldsymbol{M}}_1 - \boldsymbol{M}_1\|\right)\sigma_1. \tag{65}$$

When $r \gg K$, according to Lemmas 7, 8 and 9, we have

$$\left\|\boldsymbol{w}_j^* - |\widehat{\alpha}_j|\widehat{\boldsymbol{V}}\widehat{\boldsymbol{u}}_j\right\|_2 \lesssim \kappa^6\sqrt{\frac{K^3 r\log d}{N}}(\sigma_1 + |\xi|) \tag{66}$$

provided that $N \gtrsim r\log^4 d$.

In conclusion, we have

$$\|\boldsymbol{W}^* - \boldsymbol{W}^{(0)}\|_2 \leq \sqrt{K}\cdot\left\|\boldsymbol{w}_j^* - |\widehat{\alpha}_j|\widehat{\boldsymbol{V}}\widehat{\boldsymbol{u}}_j\right\|_2 \lesssim \kappa^6\sqrt{\frac{K^4 r\log d}{N}}(\sigma_1 + |\xi|). \tag{67}$$

□

F ADDITIONAL PROOF OF THE LEMMAS IN APPENDIX C

F.1 PROOF OF LEMMA 3

The eigenvalues of $\nabla^2 f$ at any fixed point $\boldsymbol{W}$ is bounded through the ones at the ground truth $\boldsymbol{W}^*$ by using Lemma 2. The eigenvalues of $\nabla^2 f$ at ground truth $\boldsymbol{W}^*$ is bounded in (70) and (71).

Lemma 13. *Let f be the population risk function in* (20) *and $\boldsymbol{W}$ satisfy* (6)*, then we have*

$$\|\nabla^2 f(\boldsymbol{W}) - \nabla^2 f(\boldsymbol{W}^*)\|_2 \leq \frac{4\|\boldsymbol{W}^* - \boldsymbol{W}\|_2}{\sigma_K}. \tag{68}$$

Proof of Lemma 3. Let $\lambda_{\max}(\boldsymbol{W})$ and $\lambda_{\min}(\boldsymbol{W})$ denote the largest and smallest eigenvalues of $\nabla^2 f_{\mathcal{D}}$ at point $\boldsymbol{W}$, respectively. Then, from Lemma 2, we have

$$\begin{aligned} &\lambda_{\max}(\boldsymbol{W}) \leq \lambda_{\max}(\boldsymbol{W}^*) + \|\nabla^2 f(\boldsymbol{W}) - \nabla^2 f(\boldsymbol{W}^*)\|_2, \\ \text{and}\quad &\lambda_{\min}(\boldsymbol{W}) \geq \lambda_{\min}(\boldsymbol{W}^*) - \|\nabla^2 f(\boldsymbol{W}) - \nabla^2 f(\boldsymbol{W}^*)\|_2. \end{aligned} \tag{69}$$

Next, we provide the the lower bound of Hessian of population function at ground truth $\boldsymbol{W}^*$. For any $\boldsymbol{\alpha} = [\boldsymbol{\alpha}_1^T, \boldsymbol{\alpha}_2^T, \cdots, \boldsymbol{\alpha}_K^T]^T$ with $\boldsymbol{\alpha}_j \in \mathbb{R}^r$, we have

$$\begin{aligned} \min_{\|\boldsymbol{\alpha}\|_2=1} \boldsymbol{\alpha}^T\nabla^2 f(\boldsymbol{W}^*)\boldsymbol{\alpha} &= \frac{1}{K^2}\min_{\|\boldsymbol{\alpha}\|_2=1}\mathbb{E}_{\boldsymbol{x}}\Big(\sum_{j=1}^K \boldsymbol{\alpha}_j^T\boldsymbol{x}_j\phi'(\boldsymbol{w}_j^{*T}\boldsymbol{x}_j)\Big)^2 \\ &= \frac{1}{K^2}\min_{\|\widetilde{\boldsymbol{\alpha}}\|_2=1,\ \mathrm{supp}(\widetilde{\boldsymbol{\alpha}}_j)=\mathrm{supp}(\widetilde{\boldsymbol{w}}_j^*)}\mathbb{E}_{\boldsymbol{x}}\Big(\sum_{j=1}^K \widetilde{\boldsymbol{\alpha}}_j^T\boldsymbol{x}\phi'(\widetilde{\boldsymbol{w}}_j^{*T}\boldsymbol{x})\Big)^2 \\ &\geq \frac{1}{K^2}\min_{\|\widetilde{\boldsymbol{\alpha}}\|_2=1}\mathbb{E}_{\boldsymbol{x}}\Big(\sum_{j=1}^K \widetilde{\boldsymbol{\alpha}}_j^T\boldsymbol{x}\phi'(\widetilde{\boldsymbol{w}}_j^{*T}\boldsymbol{x})\Big)^2 \\ &\geq \frac{\rho}{11\kappa^2\lambda K^2}, \end{aligned} \tag{70}$$

where $\widetilde{\boldsymbol{\alpha}} \in \mathbb{R}^{Kd}$ with $\widetilde{\boldsymbol{\alpha}}_j \in \mathbb{R}^d$, and the last inequality comes from Lemma D.6 (Zhong et al., 2017).

Next, the upper bound of Hessian of population function at ground truth $\boldsymbol{W}^*$ can be bounded in the following way. For any $\boldsymbol{\alpha}$, we have

$$\begin{aligned}\boldsymbol{\alpha}^T\nabla^2 f(\boldsymbol{W}^*)\boldsymbol{\alpha} = \frac{1}{K^2}\mathbb{E}_{\boldsymbol{x}}\Big(\sum_{j=1}^K \boldsymbol{\alpha}_j^T\boldsymbol{x}_j\phi'(\boldsymbol{w}_j^{*T}\boldsymbol{x}_j)\Big)^2 \leq& \frac{2}{K^2}\cdot\mathbb{E}_{\boldsymbol{x}}\sum_{j=1}^K\Big(\boldsymbol{\alpha}_j^T\boldsymbol{x}_j\phi'(\boldsymbol{w}_j^{*T}\boldsymbol{x}_j)\Big)^2\\ =&\frac{2}{K^2}\sum_{j=1}^K\mathbb{E}_{\boldsymbol{x}}\Big(\boldsymbol{\alpha}_j^T\boldsymbol{x}_j\phi'(\boldsymbol{w}_j^{*T}\boldsymbol{x}_j)\Big)^2\\ \leq&\frac{2}{K^2}\sum_{j=1}^K\Big(\mathbb{E}_{\boldsymbol{x}}(\boldsymbol{\alpha}_j^T\boldsymbol{x}_j)^4\mathbb{E}_{\boldsymbol{x}}|\phi'|^4\Big)^{\frac{1}{2}}\\ \leq&\frac{2}{K^2}\cdot K\cdot 3 = \frac{6}{K}.\end{aligned} \tag{71}$$

Then, from Lemma 13, when $\boldsymbol{W}$ satisfies (6), we have that

$$\|\nabla^2 f(\boldsymbol{W}) - \nabla^2 f(\boldsymbol{W}^*)\|_2 \leq \frac{\varepsilon_0\rho}{11\kappa^2\gamma}. \tag{72}$$

Hence, from (69) and (72), we have that

$$\frac{(1-\varepsilon_0)\rho}{11\kappa^2\gamma K^2}\boldsymbol{I} \leq \nabla^2 f(\boldsymbol{W}) \leq \frac{7}{K}\boldsymbol{I}. \tag{73}$$

□

F.2 Proof of Lemma 4

We first show that the second order derivative of $\hat{f}_{\mathcal{D}}$ is a sum of several random sub-exponential variables as shown in (80). Then, by concentration theory, i.e., Chernoff bound, we can show that the error bound of $\nabla^2\hat{f}_{\mathcal{D}}$ to its expectation.

Definition 1 (Definition 5.7, Vershynin (2010))**.** *A random variable X is called a sub-Gaussian random variable if it satisfies*

$$(\mathbb{E}|X|^p)^{1/p} \leq c_1\sqrt{p} \tag{74}$$

for all $p \geq 1$ and some constant $c_1 > 0$. In addition, we have

$$\mathbb{E}e^{s(X-\mathbb{E}X)} \leq e^{c_2\|X\|_{\psi_2}^2 s^2} \tag{75}$$

for all $s \in \mathbb{R}$ and some constant $c_2 > 0$, where $\|X\|_{\phi_2}$ is the sub-Gaussian norm of X defined as $\|X\|_{\psi_2} = \sup_{p\geq 1} p^{-1/2}(\mathbb{E}|X|^p)^{1/p}$.

Moreover, a random vector $\boldsymbol{X} \in \mathbb{R}^d$ belongs to the sub-Gaussian distribution if one-dimensional marginal $\boldsymbol{\alpha}^T\boldsymbol{X}$ is sub-Gaussian for any $\boldsymbol{\alpha} \in \mathbb{R}^d$, and the sub-Gaussian norm of $\boldsymbol{X}$ is defined as $\|\boldsymbol{X}\|_{\psi_2} = \sup_{\|\boldsymbol{\alpha}\|_2=1}\|\boldsymbol{\alpha}^T\boldsymbol{X}\|_{\psi_2}$.

Definition 2 (Definition 5.13, Vershynin (2010))**.** *A random variable X is called a sub-exponential random variable if it satisfies*

$$(\mathbb{E}|X|^p)^{1/p} \leq c_3 p \tag{76}$$

for all $p \geq 1$ and some constant $c_3 > 0$. In addition, we have

$$\mathbb{E}e^{s(X-\mathbb{E}X)} \leq e^{c_4\|X\|_{\psi_1}^2 s^2} \tag{77}$$

for $s \leq 1/\|X\|_{\psi_1}$ and some constant $c_4 > 0$, where $\|X\|_{\psi_1}$ is the sub-exponential norm of X defined as $\|X\|_{\psi_1} = \sup_{p\geq 1} p^{-1}(\mathbb{E}|X|^p)^{1/p}$.

Proof of Lemma 4. Recall the definition of f and $\hat{f}$ in (20) and (19), we have

$$\begin{aligned}&\frac{\partial^2 f}{\partial \boldsymbol{w}_{j_1}\partial \boldsymbol{w}_{j_2}} - \frac{\partial^2 \hat{f}_{\mathcal{D}}}{\partial \boldsymbol{w}_{j_1}\partial \boldsymbol{w}_{j_2}} \\ =&\mathbb{E}_{\boldsymbol{x}}\Big[\phi'(\boldsymbol{w}_{j_1}^T\boldsymbol{x}_{\Omega_{j_1}})\phi'(\boldsymbol{w}_{j_2}^T\boldsymbol{x}_{\Omega_{j_2}})\boldsymbol{x}_{\Omega_{j_1}}\boldsymbol{x}_{\Omega_{j_2}}^T - \frac{1}{N}\sum_{n=1}^N \phi(\boldsymbol{w}_{j_1}^T\boldsymbol{x}_{n,\Omega_{j_1}})\phi'(\boldsymbol{w}_{j_2}^T\boldsymbol{x}_{n,\Omega_{j_2}})\boldsymbol{x}_{n,\Omega_{j_1}}\boldsymbol{x}_{n,\Omega_{j_2}}^T\Big].\end{aligned} \tag{78}$$

For any $\boldsymbol{\alpha}$, we have

$$\begin{aligned}\|\nabla^2 f - \nabla^2 \hat{f}_{\mathcal{D}}\|_2 =& \max_{\|\boldsymbol{\alpha}\|_2=1}\Big|\boldsymbol{\alpha}^T(\nabla^2 f - \nabla^2 \hat{f}_{\mathcal{D}})\boldsymbol{\alpha}\Big| \\ =&\sum_{j_1=1}^K\sum_{j_2=1}^K \max_{\|\boldsymbol{\alpha}\|_2=1}\Big|\boldsymbol{\alpha}_{j_1}^T\Big(\frac{\partial^2 f}{\partial \boldsymbol{w}_{j_1}\partial \boldsymbol{w}_{j_2}} - \frac{\partial^2 \hat{f}_{\mathcal{D}}}{\partial \boldsymbol{w}_{j_1}\partial \boldsymbol{w}_{j_2}}\Big)\boldsymbol{\alpha}_{j_2}\Big| \\ =&\frac{1}{K^2}\sum_{j_1=1}^K\sum_{j_2=1}^K \max_{\|\boldsymbol{\alpha}\|_2=1}\mathbb{E}_{\boldsymbol{x}}\Big[\phi'(\boldsymbol{w}_{j_1}^T\boldsymbol{x}_{\Omega j_1})\phi'(\boldsymbol{w}_{j_2}^T\boldsymbol{x}_{\Omega j_2})\boldsymbol{\alpha}_{j_1}^T\boldsymbol{x}_{\Omega j_1}\boldsymbol{\alpha}_{j_2}^T\boldsymbol{x}_{\Omega j_2} \\ &- \frac{1}{N}\sum_{n=1}^N \phi(\boldsymbol{w}_{j_1}^T\boldsymbol{x}_{n,\Omega j_1})\phi'(\boldsymbol{w}_{j_2}^T\boldsymbol{x}_{n,\Omega j_2})\boldsymbol{\alpha}_{j_1}^T\boldsymbol{x}_{n,\Omega j_1}\boldsymbol{\alpha}_{j_2}^T\boldsymbol{x}_{n,\Omega j_2}\Big].\end{aligned} \tag{79}$$

Then, define $Z_n(j_1, j_2) = \phi(\boldsymbol{w}_{j_1}^T\boldsymbol{x}_{n,\Omega j_1})\phi'(\boldsymbol{w}_{j_2}^T\boldsymbol{x}_{n,\Omega j_2})\boldsymbol{\alpha}_{j_1}^T\boldsymbol{x}_{n,\Omega j_1}\boldsymbol{\alpha}_{j_2}^T\boldsymbol{x}_{n,\Omega j_2}$, and we say Z belongs to sub-Exponential distribution. According to Definition 2, we have

$$\begin{aligned}\big(\mathbb{E}|Z_n|^p\big)^{1/p} \leq& \bigg(\mathbb{E}\Big|\big(\boldsymbol{\alpha}_{j_1}^T\boldsymbol{x}_{n,\Omega j_1}\big)\cdot\big(\boldsymbol{\alpha}_{j_2}^T\boldsymbol{x}_{n,\Omega j_2}\big)\Big|^p\bigg)^{1/p} \\ \leq& \bigg(\mathbb{E}\Big|\big(\boldsymbol{\alpha}_{j_1}^T\boldsymbol{x}_{n,\Omega j_1}\big)\Big|^{2p}\bigg)^{1/(2p)}\cdot\bigg(\mathbb{E}\Big|\big(\boldsymbol{\alpha}_{j_2}^T\boldsymbol{x}_{n,\Omega j_2}\big)\Big|^{2p}\bigg)^{1/(2p)} \\ \leq& C_{\boldsymbol{x}}\cdot\sqrt{2p}\cdot C_{\boldsymbol{x}}\sqrt{2p} \\ =& 2C_{\boldsymbol{x}}^2\cdot p.\end{aligned} \tag{80}$$

Then, we have

$$\mathbb{E}_{Z_n} e^{s(Z_n - \mathbb{E}Z_n)} \leq e^{-Cs^2} \tag{81}$$

for some constant $C > 0$ and any $s \in \mathbb{R}$. From Chernoff bound, we have

$$\text{Prob}\Big\{\Big|\frac{1}{N}\sum_{n=1}^N(Z_n - \mathbb{E}Z_n)\Big| < t\Big\} \leq 1 - \frac{e^{-Cs^2}}{e^{st}}. \tag{82}$$

Let us select $t = \sqrt{\frac{r\log d}{N}}$ and $s = \frac{C}{2}\cdot t$, then we have

$$\Big|\frac{1}{N}\sum_{n=1}^N(Z_n - \mathbb{E}Z_n)\Big| \lesssim \sqrt{\frac{r\log d}{N}} \tag{83}$$

with probability at least $1 - d^{-C}$.

Hence, we have

$$\max_{\|\boldsymbol{\alpha}\|_2=1} \left| \boldsymbol{\alpha}_{j_1}^T \Big(\frac{\partial^2 f}{\partial \boldsymbol{w}_{j_1} \partial \boldsymbol{w}_{j_2}} - \frac{\partial^2 \hat{f}_\Omega}{\partial \boldsymbol{w}_{j_1} \partial \boldsymbol{w}_{j_2}} \Big) \boldsymbol{\alpha}_{j_2} \right| \lesssim \sqrt{\frac{r \log d}{N}}, \tag{84}$$

and

$$\|\nabla^2 f(\boldsymbol{W}) - \nabla^2 \hat{f}_\Omega(\boldsymbol{W})\|_2 \lesssim \sqrt{\frac{r \log d}{N}} \tag{85}$$

with probability at least $1 - d^{-r}$. □

G PROOF OF LEMMA 5

Proof of Lemma 5. The first-order derivative of the empirical risk function is written as

$$\begin{aligned} \frac{\partial \hat{f}_{\mathcal{D}}}{\partial \boldsymbol{w}_k} =& \frac{1}{K \cdot N} \sum_{n=1}^N \Big(y_n - \frac{1}{K} \sum_{j=1}^K \phi(\boldsymbol{w}_j^T \boldsymbol{x}_{n,\Omega_j}) \Big) \boldsymbol{x}_{n,\Omega_j} \phi'(\boldsymbol{w}_k^T \boldsymbol{x}_{n,\Omega_j}) \\ =& \frac{1}{K^2 \cdot N} \sum_{n=1}^N \sum_{j=1}^K \big(\phi(\boldsymbol{w}_j^{*T} \boldsymbol{x}_{n,\Omega_j}) - \phi(\boldsymbol{w}_j^T \boldsymbol{x}_{n,\Omega_j}) \big) \boldsymbol{x}_{n,\Omega_j} \phi'(\boldsymbol{w}_k^T \boldsymbol{x}_{n,\Omega_j}) \\ &+ \frac{1}{K^2 \cdot N} \sum_{j=1}^K \xi_n \boldsymbol{x}_{n,\Omega_j} \phi'(\boldsymbol{w}_k^T \boldsymbol{x}_{n,\Omega_j}) \end{aligned} \tag{86}$$

Define $\boldsymbol{z}_n(j,k) = \big(\phi(\boldsymbol{w}_j^{*T} \boldsymbol{x}_{n,\Omega_j}) - \phi(\boldsymbol{w}_j^T \boldsymbol{x}_{n,\Omega_j}) \big) \phi'(\boldsymbol{w}_k^T \boldsymbol{x}_{n,\Omega_j}) \boldsymbol{x}_{n,\Omega_j}$. Then, for any $\boldsymbol{\alpha}_j \in \mathbb{R}^r$, we have

$$\begin{aligned} p^{-1} \Big(\mathbb{E}_{\boldsymbol{x}} \big| \boldsymbol{\alpha}_j^T \boldsymbol{z}_n \big|^p \Big)^{\frac{1}{p}} =& p^{-1} \Big(\mathbb{E}_{\boldsymbol{x}} \big| (\boldsymbol{\alpha}_j^T \boldsymbol{x}_{n,\Omega_j}) \big(\phi(\boldsymbol{w}_j^{*T} \boldsymbol{x}_{n,\Omega_j}) - \phi(\boldsymbol{w}_j^T \boldsymbol{x}_{n,\Omega_j}) \big) \phi'(\boldsymbol{w}_k^T \boldsymbol{x}_{n,\Omega_j}) \big|^p \Big)^{\frac{1}{p}} \\ \le& p^{-1} \Big(\mathbb{E}_{\boldsymbol{x}} \big| (\boldsymbol{\alpha}_j^T \boldsymbol{x}_{n,\Omega_j}) \big(\phi(\boldsymbol{w}_j^{*T} \boldsymbol{x}_{n,\Omega_j}) - \phi(\boldsymbol{w}_j^T \boldsymbol{x}_{n,\Omega_j}) \big) \big|^p \Big)^{\frac{1}{p}} \\ \le& p^{-1} \big(\mathbb{E}_{\boldsymbol{x}} |\boldsymbol{\alpha}_j^T \boldsymbol{x}_{n,\Omega_j}|^{2p} \big)^{\frac{1}{2p}} \cdot \Big(\mathbb{E}_{\boldsymbol{x}} \big| \phi(\boldsymbol{w}_j^{*T} \boldsymbol{x}_{n,\Omega_j}) - \phi(\boldsymbol{w}_j^T \boldsymbol{x}_{n,\Omega_j}) \big|^{2p} \Big)^{\frac{1}{2p}} \\ \le& p^{-1} \big(\mathbb{E}_{\boldsymbol{x}} |\boldsymbol{\alpha}_j^T \boldsymbol{x}_{n,\Omega_j}|^{2p} \big)^{\frac{1}{2p}} \cdot \Big(\mathbb{E}_{\boldsymbol{x}} \big| (\boldsymbol{w}_j^* - \boldsymbol{w}_j)^T \boldsymbol{x}_{n,\Omega_j} \big|^{2p} \Big)^{\frac{1}{2p}} \\ \le& 2 \|\boldsymbol{w}_j^* - \boldsymbol{w}_j\|_2. \end{aligned} \tag{87}$$

Following similar steps in (82), by Chernoff bound, we have

$$\Big\| \frac{1}{N} \sum_{n=1}^N (\boldsymbol{z}_n - \mathbb{E}_{\boldsymbol{x}} \boldsymbol{z}_n) \Big\|_2 \lesssim \sqrt{\frac{r \log d}{N}} \cdot \|\boldsymbol{w}_j^* - \boldsymbol{w}_j\|_2 \tag{88}$$

with probability at least $1 - d^{-r}$. Also, we know that $\boldsymbol{x}_{n,\Omega_j} \phi'(W_k^T \boldsymbol{x}_{n,\Omega_j})$ belongs to sub-Gaussian distribution as well. Then, by Chernoff bound, we have

$$\begin{aligned} \Big\| \frac{1}{N} \sum_{n=1}^N \xi_n \boldsymbol{x}_{n,\Omega_j} \phi'(\boldsymbol{w}_j^T \boldsymbol{x}_{n,\Omega_j}) \Big\|_2 \lesssim& |\xi| \cdot \Big\| \frac{1}{N} \sum_{n=1}^N \boldsymbol{x}_{n,\Omega_j} \phi'(\boldsymbol{w}_j^T \boldsymbol{x}_{n,\Omega_j}) \Big\|_2 \\ \lesssim& |\xi| \cdot \sqrt{\frac{r \log d}{N}} \end{aligned} \tag{89}$$

with probability at least $1 - d^{-r}$. □

H PROOF OF LEMMA 13

Proof of Lemma 13. Recall the definition of population risk function, we have

$$\frac{\partial^2 f(\boldsymbol{W}^*)}{\partial \boldsymbol{w}_{j_1}\partial \boldsymbol{w}_{j_2}} = \frac{1}{K^2}\mathbb{E}_{\boldsymbol{x}}\phi'(\boldsymbol{w}_{j_1}^{*T}\boldsymbol{x}_{\Omega j_1})\phi'(\boldsymbol{w}_{j_2}^{*T}\boldsymbol{x}_{\Omega j_2})\boldsymbol{x}_{\Omega j_1}\boldsymbol{x}_{\Omega j_2}^T \tag{90}$$

and

$$\frac{\partial^2 f(\boldsymbol{W})}{\partial \boldsymbol{w}_{j_1}\partial \boldsymbol{w}_{j_2}} = \frac{1}{K^2}\mathbb{E}_{\boldsymbol{x}}\phi'(\boldsymbol{w}_{j_1}^{T}\boldsymbol{x}_{\Omega j_1})\phi'(\boldsymbol{w}_{j_2}^{T}\boldsymbol{x}_{\Omega j_2})\boldsymbol{x}_{\Omega j_1}\boldsymbol{x}_{\Omega j_2}^T \tag{91}$$

Then, we have

$$\begin{aligned}
&\frac{\partial^2 f(\boldsymbol{W}^*)}{\partial \boldsymbol{w}_{j_1}\partial \boldsymbol{w}_{j_2}} - \frac{\partial^2 f(\boldsymbol{W})}{\partial \boldsymbol{w}_{j_1}\partial \boldsymbol{w}_{j_2}} \\
=&\frac{1}{K^2}\mathbb{E}_{\boldsymbol{x}}\Big[\phi'(\boldsymbol{w}_{j_1}^{*T}\boldsymbol{x}_{\Omega j_1})\phi'(\boldsymbol{w}_{j_2}^{*T}\boldsymbol{x}_{\Omega j_2}) - \phi'(\boldsymbol{w}_{j_1}^{T}\boldsymbol{x}_{\Omega j_1})\phi'(\boldsymbol{w}_{j_2}^{T}\boldsymbol{x}_{\Omega j_2})\Big]\boldsymbol{x}_{\Omega j_1}\boldsymbol{x}_{\Omega j_2}^T \\
=&\frac{1}{K^2}\mathbb{E}_{\boldsymbol{x}}\Big[\phi'(\boldsymbol{w}_{j_1}^{*T}\boldsymbol{x}_{\Omega j_1})\big(\phi'(\boldsymbol{w}_{j_2}^{*T}\boldsymbol{x}_{\Omega j_2}) - \phi'(\boldsymbol{w}_{j_2}^{T}\boldsymbol{x}_{\Omega j_2})\big) + \phi'(\boldsymbol{w}_{j_2}^{T}\boldsymbol{x}_{\Omega j_2})\big(\phi'(\boldsymbol{w}_{j_1}^{*T}\boldsymbol{x}_{\Omega j_1}) - \phi'(\boldsymbol{w}_{j_1}^{T}\boldsymbol{x}_{\Omega j_1})\big)\Big]\boldsymbol{x}_{\Omega j_1}\boldsymbol{x}_{\Omega j_2}^T \\
=&\frac{1}{K^2}\Big[\mathbb{E}_{\boldsymbol{x}}\phi'(\boldsymbol{w}_{j_1}^{*T}\boldsymbol{x}_{\Omega j_1})\big(\phi'(\boldsymbol{w}_{j_2}^{*T}\boldsymbol{x}_{\Omega j_2}) - \phi'(\boldsymbol{w}_{j_2}^{T}\boldsymbol{x}_{\Omega j_2})\big)\boldsymbol{x}_{\Omega j_1}\boldsymbol{x}_{\Omega j_2}^T \\
&+\mathbb{E}_{\boldsymbol{x}}\phi'(\boldsymbol{w}_{j_2}^{T}\boldsymbol{x}_{\Omega j_2})\big(\phi'(\boldsymbol{w}_{j_1}^{*T}\boldsymbol{x}_{\Omega j_1}) - \phi'(\boldsymbol{w}_{j_1}^{T}\boldsymbol{x}_{\Omega j_1})\big)\boldsymbol{x}_{\Omega j_1}\boldsymbol{x}_{\Omega j_2}^T\Big] \\
:=&\frac{1}{K^2}(\boldsymbol{I}_1 + \boldsymbol{I}_2).
\end{aligned} \tag{92}$$

For any $\boldsymbol{\alpha}_{j_1}$ and $\boldsymbol{\alpha}_{j_2} \in \mathbb{R}^r$, we have

$$\begin{aligned}
&\max_{\|\boldsymbol{\alpha}_{j_1}\|_2, \|\boldsymbol{\alpha}_{j_2}\|_2=1} \boldsymbol{\alpha}_{j_1}^T\boldsymbol{I}_1\boldsymbol{\alpha}_{j_2} \\
=&\max_{\|\boldsymbol{\alpha}_{j_1}\|_2, \|\boldsymbol{\alpha}_{j_2}\|_2=1} \mathbb{E}_{\boldsymbol{x}}\phi'(\boldsymbol{w}_{j_1}^{*T}\boldsymbol{x}_{\Omega j_1})\big(\phi'(\boldsymbol{w}_{j_2}^{*T}\boldsymbol{x}_{\Omega j_2}) - \phi'(\boldsymbol{w}_{j_2}^{T}\boldsymbol{x}_{\Omega j_2})\big)\cdot(\boldsymbol{\alpha}_{j_1}^T\boldsymbol{x}_{\Omega j_1})\cdot(\boldsymbol{\alpha}_{j_2}^T\boldsymbol{x}_{\Omega j_2}) \\
\le&\max_{\|\boldsymbol{a}\|_2=1} \mathbb{E}_{\boldsymbol{x}}\phi'(\widetilde{\boldsymbol{w}}_{j_1}^{*T}\boldsymbol{x})\big(\phi'(\widetilde{\boldsymbol{w}}_{j_2}^{*T}\boldsymbol{x}) - \phi'(\widetilde{\boldsymbol{w}}_{j_2}^{T}\boldsymbol{x})\big)\cdot(\boldsymbol{a}^T\boldsymbol{x})^2,
\end{aligned} \tag{93}$$

where $\boldsymbol{a} \in \mathbb{R}^d$. Let $I = \phi'(\widetilde{\boldsymbol{w}}_{j_1}^{*T}\boldsymbol{x})\big(\phi'(\widetilde{\boldsymbol{w}}_{j_2}^{*T}\boldsymbol{x}) - \phi'(\widetilde{\boldsymbol{w}}_{j_2}^{T}\boldsymbol{x})\big)\cdot(\boldsymbol{a}^T\boldsymbol{x})^2$. It is easy to verify there exists a basis such that $\mathcal{B} = \{\boldsymbol{a}, \boldsymbol{b}, \boldsymbol{c}, \boldsymbol{a}_4^\perp, \cdots, \boldsymbol{a}_d^\perp\}$ with $\{\boldsymbol{a}, \boldsymbol{b}, \boldsymbol{c}\}$ spans a subspace that contains $\boldsymbol{a}, \boldsymbol{w}_{j_2}$ and $\boldsymbol{w}_{j_2}^*$. Then, for any $\boldsymbol{x}$, we have a unique $\boldsymbol{z} = \begin{bmatrix} z_1 & z_2 & \cdots & z_d \end{bmatrix}^T$ such that

$$\boldsymbol{x} = z_1\boldsymbol{a} + z_2\boldsymbol{b} + z_3\boldsymbol{c} + \cdots + z_d\boldsymbol{a}_d^\perp.$$

Also, since $\boldsymbol{x} \sim \mathcal{N}(\boldsymbol{0}, \boldsymbol{I}_d)$, we have $\boldsymbol{z} \sim \mathcal{N}(\boldsymbol{0}, \boldsymbol{I}_d)$. Then, we have

$$\begin{aligned}
I =&\mathbb{E}_{z_1,z_2,z_3}|\phi'\big(\widetilde{\boldsymbol{w}}_{j_2}^{T}\boldsymbol{x}\big) - \phi'\big(\widetilde{\boldsymbol{w}}_{j_2}^{*T}\boldsymbol{x}\big)|\cdot|\boldsymbol{a}^T\boldsymbol{x}|^2 \\
=&\int |\phi'\big(\widetilde{\boldsymbol{w}}_{j_2}^{T}\boldsymbol{x}\big) - \phi'\big(\widetilde{\boldsymbol{w}}_{j_2}^{*T}\boldsymbol{x}\big)|\cdot|\boldsymbol{a}^T\boldsymbol{x}|^2\cdot f_Z(z_1,z_2,z_3)dz_1dz_2dz_3,
\end{aligned}$$

where $\boldsymbol{x} = z_1\boldsymbol{a} + z_2\boldsymbol{b} + z_3\boldsymbol{c}$ and $f_Z(z_1, z_2, z_3)$ is probability density function of (z_1, z_2, z_3). Next, we consider spherical coordinates with $z_1 = rcos\phi_1, z_2 = rsin\phi_1 sin\phi_2, z_3 = z_2 = rsin\phi_1 cos\phi_2$. Hence,

$$I = \int |\phi'\big(\widetilde{\boldsymbol{w}}_{j_2}^{T}\boldsymbol{x}\big) - \phi'\big(\widetilde{\boldsymbol{w}}_{j_2}^{*T}\boldsymbol{x}\big)|\cdot|r\cos\phi_1|^2\cdot\cdot f_Z(r,\phi_1,\phi_2)r^2\sin\phi_1 drd\phi_1 d\phi_2. \tag{94}$$

It is easy to verify that $\phi'\big(\boldsymbol{w}_{j_2}^T\boldsymbol{x}\big)$ only depends on the direction of $\boldsymbol{x}$ and

$$f_Z(r,\phi_1,\phi_2)=\frac{1}{(2\pi)^{\frac{3}{2}}}e^{\frac{x_1^2+x_2^2+x_3^2}{2}}=\frac{1}{(2\pi)^{\frac{3}{2}}}e^{\frac{r^2}{2}}$$

only depends on r. Then, we have

$$\begin{aligned}
I(i_2,j_2)=&\int|\phi'\big(\widetilde{\boldsymbol{w}}_{j_2}^T(\boldsymbol{x}/r)\big)-\phi'\big(\widetilde{\boldsymbol{w}}_{j_2}^{*T}(\boldsymbol{x}/r)\big)|\cdot|r\cos\phi_1|^2\cdot f_Z(r)r^2\sin\phi_1 drd\phi_1d\phi_2\\
=&\int_0^\infty r^4f_z(r)dr\int_0^\pi\int_0^{2\pi}|\cos\phi_1|^2\cdot\sin\phi_1\cdot|\phi'\big(\widetilde{\boldsymbol{w}}_{j_2}^T(\boldsymbol{x}/r)\big)-\phi'\big(\widetilde{\boldsymbol{w}}_{j_2}^{*T}(\boldsymbol{x}/r)\big)|d\phi_1d\phi_2\\
\leq&\sqrt{\frac{8}{\pi}}\int_0^\infty r^2f_z(r)dr\int_0^\pi\int_0^{2\pi}\sin\phi_1\cdot|\phi'\big(\widetilde{\boldsymbol{w}}_{j_2}^T(\boldsymbol{x}/r)\big)-\phi'\big(\widetilde{\boldsymbol{w}}_{j_2}^{*T}(\boldsymbol{x}/r)\big)|d\phi_1d\phi_2\\
=&\sqrt{\frac{8}{\pi}}\mathbb{E}_{z_1,z_2,z_3}\big|\phi'\big(\widetilde{\boldsymbol{w}}_{j_2}^T\boldsymbol{x}\big)-\phi'\big(\widetilde{\boldsymbol{w}}_{j_2}^{*T}\boldsymbol{x}\big)|\\
=&\sqrt{\frac{8}{\pi}}\mathbb{E}_{\boldsymbol{x}}\big|\phi'\big(\widetilde{\boldsymbol{w}}_{j_2}^T\boldsymbol{x}\big)-\phi'\big(\widetilde{\boldsymbol{w}}_{j_2}^{*T}\boldsymbol{x}\big)|.
\end{aligned}\tag{95}$$

Define a set $\mathcal{A}_1=\{\boldsymbol{x}|(\widetilde{\boldsymbol{w}}_{j_2}^{*T}\boldsymbol{x})(\widetilde{\boldsymbol{w}}_{j_2}^T\boldsymbol{x})<0\}$. If $\boldsymbol{x}\in\mathcal{A}_1$, then $\widetilde{\boldsymbol{w}}_{j_2}^{*T}\boldsymbol{x}$ and $\widetilde{\boldsymbol{w}}_{j_2}^T\boldsymbol{x}$ have different signs, which means the value of $\phi'(\widetilde{\boldsymbol{w}}_{j_2}^T\boldsymbol{x})$ and $\phi'(\widetilde{\boldsymbol{w}}_{j_2}^{*T}\boldsymbol{x})$ are different. This is equivalent to say that

$$|\phi'(\boldsymbol{w}_{j_2}^T\boldsymbol{x})-\phi'(\boldsymbol{w}_{j_2}^{*\ T}\boldsymbol{x})|=\begin{cases}1,\ \text{if }\boldsymbol{x}\in\mathcal{A}_1\\0,\ \text{if }\boldsymbol{x}\in\mathcal{A}_1^c\end{cases}.\tag{96}$$

Moreover, if $\boldsymbol{x}\in\mathcal{A}_1$, then we have

$$|\boldsymbol{w}_{j_2}^{*\ T}\boldsymbol{x}|\leq|\widetilde{\boldsymbol{w}}_{j_2}^{*T}\boldsymbol{x}-\widetilde{\boldsymbol{w}}_{j_2}^T\boldsymbol{x}|\leq\|\widetilde{\boldsymbol{w}}_{j_2}^*-\widetilde{\boldsymbol{w}}_{j_2}\|\cdot\|\boldsymbol{x}\|.\tag{97}$$

Define a set $\mathcal{A}_2$ such that

$$\mathcal{A}_2=\Big\{\boldsymbol{x}\Big|\frac{|\widetilde{\boldsymbol{w}}_{j_2}^{*T}\boldsymbol{x}|}{\|\widetilde{\boldsymbol{w}}_{j_2}^*\|\|\boldsymbol{x}\|}\leq\frac{\|\widetilde{\boldsymbol{w}}_{j_2}^*-\widetilde{\boldsymbol{w}}_{j_2}\|}{\|\widetilde{\boldsymbol{w}}_{j_2}^*\|}\Big\}=\Big\{\theta_{\boldsymbol{x},\boldsymbol{w}_{j_2}^*}\Big||\cos\theta_{\boldsymbol{x},\widetilde{\boldsymbol{w}}_{j_2}^*}|\leq\frac{\|\widetilde{\boldsymbol{w}}_{j_2}^*-\widetilde{\boldsymbol{w}}_{j_2}\|}{\|\widetilde{\boldsymbol{w}}_{j_2}^*\|}\Big\}.\tag{98}$$

Hence, we have that

$$\begin{aligned}
\mathbb{E}_{\boldsymbol{x}}|\phi'(\widetilde{\boldsymbol{w}}_{j_2}^T\boldsymbol{x})-\phi'(\widetilde{\boldsymbol{w}}_{j_2}^{*T}\boldsymbol{x})|^2=&\mathbb{E}_{\boldsymbol{x}}|\phi'(\widetilde{\boldsymbol{w}}_{j_2}^T\boldsymbol{x})-\phi'(\widetilde{\boldsymbol{w}}_{j_2}^{*T}\boldsymbol{x})|\\
=&\text{Prob}(\boldsymbol{x}\in\mathcal{A}_1)\\
\leq&\text{Prob}(\boldsymbol{x}\in\mathcal{A}_2).
\end{aligned}\tag{99}$$

Since $\boldsymbol{x}\sim\mathcal{N}(\boldsymbol{0},\boldsymbol{I})$, $\theta_{\boldsymbol{x},\boldsymbol{w}_{j_2}^*}$ belongs to the uniform distribution on $[-\pi,\pi]$, we have

$$\begin{aligned}
\text{Prob}(\boldsymbol{x}\in\mathcal{A}_2)=\frac{\pi-\arccos\frac{\|\widetilde{\boldsymbol{w}}_{j_2}^*-\widetilde{\boldsymbol{w}}_{j_2}\|}{\|\widetilde{\boldsymbol{w}}_{j_2}^*\|}}{\pi}\leq&\frac{1}{\pi}\tan(\pi-\arccos\frac{\|\widetilde{\boldsymbol{w}}_{j_2}^*-\widetilde{\boldsymbol{w}}_{j_2}\|}{\|\widetilde{\boldsymbol{w}}_{j_2}^*\|})\\
=&\frac{1}{\pi}\cot(\arccos\frac{\|\widetilde{\boldsymbol{w}}_{j_2}^*-\widetilde{\boldsymbol{w}}_{j_2}\|}{\|\widetilde{\boldsymbol{w}}_{j_2}^*\|})\\
\leq&\frac{2}{\pi}\frac{\|\widetilde{\boldsymbol{w}}_{j_2}^*-\widetilde{\boldsymbol{w}}_{j_2}\|}{\|\widetilde{\boldsymbol{w}}_{j_2}^*\|}\\
=&\frac{2}{\pi}\frac{\|\boldsymbol{w}_{j_2}^*-\boldsymbol{w}_{j_2}\|}{\|\boldsymbol{w}_{j_2}^*\|}.
\end{aligned}\tag{100}$$

Hence, (95) and (100) suggest that

$$I \leq \frac{6}{\pi} \frac{\|\boldsymbol{w}_{j_2}^* - \boldsymbol{w}_{j_2}\|_2}{\|\boldsymbol{w}_{j_2}^*\|_2}. \tag{101}$$

The same bound that shown in (101) holds for $\boldsymbol{I}_2$ as well. □

I ADDITIONAL PROOFS OF LEMMAS IN APPENDIX E

I.1 ERROR BOUND FOR THE SECOND-ORDER MOMENT

Proof of Lemma 7. Let us define

$$\widetilde{\boldsymbol{x}_n} = \frac{1}{\sqrt{K}} \sum_{j=1}^{K} \boldsymbol{x}_{n,\Omega_j}. \tag{102}$$

Then, for $\widehat{\boldsymbol{M}}_2 - \boldsymbol{M}_2$, we have

$$\begin{aligned}
&\widehat{\boldsymbol{M}}_2 - \boldsymbol{M}_2 \\
=&\frac{1}{N} \sum_{n=1}^{N} y_n (\widetilde{\boldsymbol{x}}_n \otimes \widetilde{\boldsymbol{x}}_n - \mathbb{E}\widetilde{\boldsymbol{x}}_n \widetilde{\boldsymbol{x}}_n^T) - \mathbb{E}_{\boldsymbol{x}}\, y(\widetilde{\boldsymbol{x}} \otimes \widetilde{\boldsymbol{x}} - \mathbb{E}\widetilde{\boldsymbol{x}}\widetilde{\boldsymbol{x}}^T) \\
=&\frac{1}{N} \sum_{n=1}^{N} \big(\frac{1}{K} \sum_{j=1}^{K} \phi(\boldsymbol{w}_j^{*T} \boldsymbol{x}_{n,\Omega_j} + \xi_n)\big)(\widetilde{\boldsymbol{x}}_n \otimes \widetilde{\boldsymbol{x}}_n - \mathbb{E}\widetilde{\boldsymbol{x}}_n \widetilde{\boldsymbol{x}}_n^T) \\
&- \mathbb{E}_{\boldsymbol{x}}\, \frac{1}{K} \sum_{j=1}^{K} \phi(\boldsymbol{w}_j^{*T} \boldsymbol{x}_{\Omega_j})(\widetilde{\boldsymbol{x}} \otimes \widetilde{\boldsymbol{x}} - \mathbb{E}\widetilde{\boldsymbol{x}}\widetilde{\boldsymbol{x}}^T) \\
=&\frac{1}{K \cdot N} \sum_{n=1}^{N} \sum_{j=1}^{K} \Big(\phi(\boldsymbol{w}_j^{*T} \boldsymbol{x}_{n,\Omega_j})(\widetilde{\boldsymbol{x}}_n \otimes \widetilde{\boldsymbol{x}}_n - \mathbb{E}\widetilde{\boldsymbol{x}}_n \widetilde{\boldsymbol{x}}_n^T) - \mathbb{E}_{\boldsymbol{x}}\, \phi(\boldsymbol{w}_j^{*T} \boldsymbol{x}_{\Omega_j})(\widetilde{\boldsymbol{x}} \otimes \widetilde{\boldsymbol{x}} - \mathbb{E}\widetilde{\boldsymbol{x}}\widetilde{\boldsymbol{x}}^T)\Big) \\
&+ \frac{1}{N} \sum_{n=1}^{N} \xi_n (\widetilde{\boldsymbol{x}}_n \otimes \widetilde{\boldsymbol{x}}_n - \mathbb{E}\widetilde{\boldsymbol{x}}_n \widetilde{\boldsymbol{x}}_n^T)
\end{aligned} \tag{103}$$

Following the notations in Lemma E.2 of [40], we denote

$$\boldsymbol{B}_2(\boldsymbol{x}_n) := \frac{1}{K} \sum_{j=1}^{K} \phi(\boldsymbol{w}_j^{*T} \boldsymbol{x}_{n,\Omega_j})(\widetilde{\boldsymbol{x}}_n \otimes \widetilde{\boldsymbol{x}}_n - \mathbb{E}\widetilde{\boldsymbol{x}}_n \widetilde{\boldsymbol{x}}_n^T). \tag{104}$$

Following the similar calculations of (I) - (III) in Lemma E.2 [40], we know that

$$\begin{aligned}
\|\boldsymbol{B}_2(\boldsymbol{x})\|_2 &\lesssim \sigma_1 r \log^{\frac{3}{2}} d, \\
\|\mathbb{E}_{\boldsymbol{x}} \boldsymbol{B}_2(\boldsymbol{x})\|_2 &\lesssim \sigma_1, \\
\|\mathbb{E}_{\boldsymbol{x}} \boldsymbol{B}_2^2(\boldsymbol{x})\|_2 &\lesssim \sigma_1^2 r
\end{aligned} \tag{105}$$

hold with probability at least $1 - d^{-10}$.

Define $\boldsymbol{Z}_{2,n} = \frac{1}{N}\big(\boldsymbol{B}_2(\boldsymbol{x}_n) - \mathbb{E}_{\boldsymbol{x}} \boldsymbol{B}_2(\boldsymbol{x})\big)$ for $\boldsymbol{x}_n$ with $n \in [N]$, and it is obvious $\boldsymbol{Z}_n$ is zero mean. Also, we have

$$R_2 = \|\boldsymbol{Z}_{2,n}\|_2 \leq \frac{1}{N}\big(\|\boldsymbol{B}_2(\boldsymbol{x}_n)\|_2 + \|\mathbb{E}_{\boldsymbol{x}} \boldsymbol{B}_2(\boldsymbol{x})\|_2\big) \lesssim N^{-1} \sigma_1 r \log^{\frac{3}{2}} d, \tag{106}$$

and

$$\begin{aligned}\delta_2^2 = \Big\| \sum_{n=1}^N \mathbb{E}\boldsymbol{Z}_{2,n}^2 \Big\|_2^2 \leq & \Big\| \sum_{n=1}^N \frac{1}{N^2}\Big(\mathbb{E}\boldsymbol{B}_2^2(\boldsymbol{x}_n) - \big(\mathbb{E}\boldsymbol{B}_2(\boldsymbol{x}_n)\big)^2\Big)\Big\|_2 \\ \leq & \frac{1}{N}\Big(\|\mathbb{E}\boldsymbol{B}_2^2(\boldsymbol{x}_n)\|_2 + \|\mathbb{E}\boldsymbol{B}_2(\boldsymbol{x}_n)\|_2^2\Big) \\ \lesssim & N^{-1}\sigma_1^2 r.\end{aligned} \tag{107}$$

Next, let $t = \Theta(\sigma_1\sqrt{\frac{r\log d}{N}})$. To make sure $\delta_2^2 \geq R_2 t/3$, we need $N \gtrsim r\log^4 d$. Then, by Lemma 10, we have

$$\text{Prob}\Big\{\Big\|\sum_n \boldsymbol{Z}_{2,n}\Big\|_2 \geq t\Big\} \leq 2r\exp\Big(\frac{-t^2/2}{\delta^2 + Rt/3}\Big) \leq 2r\exp\Big(\frac{-t^2}{4\delta^2}\Big). \tag{108}$$

That is

$$\Big\|\sum_{n=1}^N \boldsymbol{Z}_{2,n}\Big\|_2 \lesssim \sigma_1\sqrt{\frac{r\log d}{N}} \tag{109}$$

with probability at least $1 - d^{-10}$. Because $\widetilde{\boldsymbol{x}}_n$ belongs to the sub-Gaussian distribution, we know that

$$\Big\|\frac{1}{N}\sum_{n=1}^N(\widetilde{\boldsymbol{x}}_n \otimes \widetilde{\boldsymbol{x}}_n - \mathbb{E}\widetilde{\boldsymbol{x}}_n\widetilde{\boldsymbol{x}}_n^T)\Big\|_2 \lesssim \sqrt{\frac{r\log d}{N}} \tag{110}$$

with probability at least $1 - d^{-10}$.

In conclusion, we have

$$\|\widehat{\boldsymbol{M}}_2 - \boldsymbol{M}_2\| \lesssim (\sigma_1 + |\xi|)\sqrt{\frac{r\log d}{N}} \tag{111}$$

with probability at least $1 - d^{-C}$ provided that $N \gtrsim r\log^4 d$. □

I.2 Error bound for the third-order moment

Proof of Lemma 8. For $\widehat{\boldsymbol{M}}_3(\widehat{\boldsymbol{V}},\widehat{\boldsymbol{V}},\widehat{\boldsymbol{V}})-\boldsymbol{M}_3(\widehat{\boldsymbol{V}},\widehat{\boldsymbol{V}},\widehat{\boldsymbol{V}})$, we have

$$\begin{aligned}
&\widehat{\boldsymbol{M}}_3(\widehat{\boldsymbol{V}},\widehat{\boldsymbol{V}},\widehat{\boldsymbol{V}})-\boldsymbol{M}_3(\widehat{\boldsymbol{V}},\widehat{\boldsymbol{V}},\widehat{\boldsymbol{V}})\\
=&\frac{1}{N}\sum_{n=1}^{N} y_n\big[(\widehat{\boldsymbol{V}}^T\widetilde{\boldsymbol{x}}_n)^{\otimes 3}-(\widehat{\boldsymbol{V}}^T\widetilde{\boldsymbol{x}}_n)\otimes(\mathbb{E}(\widehat{\boldsymbol{V}}^T\widetilde{\boldsymbol{x}}_n)(\widehat{\boldsymbol{V}}^T\widetilde{\boldsymbol{x}}_n)^T)\big]\\
&-\mathbb{E}_{\boldsymbol{x}}\, y\big[(\widehat{\boldsymbol{V}}^T\widetilde{\boldsymbol{x}})^{\otimes 3}-(\widehat{\boldsymbol{V}}^T\boldsymbol{x}^T)\otimes\mathbb{E}(\widehat{\boldsymbol{V}}^T\widetilde{\boldsymbol{x}}_n)(\widehat{\boldsymbol{V}}^T\widetilde{\boldsymbol{x}}_n)^T\big]\\
=&\frac{1}{N}\sum_{n=1}^{N}\Big(\frac{1}{K}\sum_{j=1}^{K}\phi(\boldsymbol{w}_j^{*T}\boldsymbol{x}_{n,\Omega_j})+\xi_n\Big)\cdot\big[(\widehat{\boldsymbol{V}}^T\widetilde{\boldsymbol{x}}_n)^{\otimes 3}-(\widehat{\boldsymbol{V}}^T\widetilde{\boldsymbol{x}}_n)\otimes(\mathbb{E}(\widehat{\boldsymbol{V}}^T\widetilde{\boldsymbol{x}}_n)(\widehat{\boldsymbol{V}}^T\widetilde{\boldsymbol{x}}_n)^T)\big]\\
&-\mathbb{E}_{\boldsymbol{x}}\,\frac{1}{K}\sum_{j=1}^{K}\phi(\boldsymbol{w}_j^{*T}\boldsymbol{x}_{\Omega_j})\big[(\widehat{\boldsymbol{V}}^T\widetilde{\boldsymbol{x}})^{\otimes 3}-(\widehat{\boldsymbol{V}}^T\widetilde{\boldsymbol{x}})\otimes(\mathbb{E}(\widehat{\boldsymbol{V}}^T\widetilde{\boldsymbol{x}})(\widehat{\boldsymbol{V}}^T\widetilde{\boldsymbol{x}})^T)\big]\\
=&\frac{1}{K\cdot N}\sum_{n=1}^{N}\sum_{j=1}^{K}\Big[\phi(\boldsymbol{w}_j^{*T}\boldsymbol{x}_{n,\Omega_j})\cdot\big[(\widehat{\boldsymbol{V}}^T\widetilde{\boldsymbol{x}}_n)^{\otimes 3}-(\widehat{\boldsymbol{V}}^T\widetilde{\boldsymbol{x}}_n)\otimes(\mathbb{E}(\widehat{\boldsymbol{V}}^T\widetilde{\boldsymbol{x}}_n)(\widehat{\boldsymbol{V}}^T\widetilde{\boldsymbol{x}}_n)^T)\big]\\
&-\mathbb{E}_{\boldsymbol{x}}\phi(\boldsymbol{w}_j^{*T}\boldsymbol{x}_{\Omega_j})\big[(\widehat{\boldsymbol{V}}^T\widetilde{\boldsymbol{x}})^{\otimes 3}-(\widehat{\boldsymbol{V}}^T\widetilde{\boldsymbol{x}})\otimes(\mathbb{E}(\widehat{\boldsymbol{V}}^T\widetilde{\boldsymbol{x}})(\widehat{\boldsymbol{V}}^T\widetilde{\boldsymbol{x}})^T)\big]\Big]\\
&+\frac{1}{N}\sum_{n=1}^{N}\xi_n\big[(\widehat{\boldsymbol{V}}^T\widetilde{\boldsymbol{x}})^{\otimes 3}-(\widehat{\boldsymbol{V}}^T\widetilde{\boldsymbol{x}})\otimes(\mathbb{E}(\widehat{\boldsymbol{V}}^T\widetilde{\boldsymbol{x}})(\widehat{\boldsymbol{V}}^T\widetilde{\boldsymbol{x}})^T)\big]
\end{aligned}\tag{112}$$

Following the notations in Lemma E.8 of [40], we define

$$\boldsymbol{T}(\boldsymbol{x}):=\frac{1}{K}\sum_{j=1}^{K}\phi(\boldsymbol{w}_j^{*T}\boldsymbol{x}_{n,\Omega_j})\cdot\big[(\widehat{\boldsymbol{V}}^T\boldsymbol{x}_n)^{\otimes 3}-(\widehat{\boldsymbol{V}}^T\boldsymbol{x}_n)\otimes(\mathbb{E}(\widehat{\boldsymbol{V}}^T\boldsymbol{x}_n)(\widehat{\boldsymbol{V}}^T\boldsymbol{x}_n)^T)\big].\tag{113}$$

Then, $\boldsymbol{B}_3(\boldsymbol{x})\in\mathbb{R}^{K\times K^2}$ is defined as flattening the tensor $\boldsymbol{T}(\boldsymbol{x})$ along the first dimension. Hence, we have

$$\begin{aligned}
\|\boldsymbol{B}_3(\boldsymbol{x})\|_2\lesssim&\max_j|\boldsymbol{w}_j^*\boldsymbol{x}_{\Omega_j}|\cdot\Big(\|\widehat{\boldsymbol{V}}^T\boldsymbol{x}_n\|_2^3+3K\|\widehat{\boldsymbol{V}}^T\boldsymbol{x}_n\|_2\Big)\\
\lesssim&\sigma_1K^{\frac{3}{2}}\log^{\frac{5}{2}}d
\end{aligned}\tag{114}$$

with probability at least $1-d^{-10}$.

Following the similar calculations of (II) and (III) in Lemma E.8 of [40], we know that

$$\begin{aligned}
&\|\mathbb{E}_{\boldsymbol{x}}\boldsymbol{B}_3(\boldsymbol{x})\|_2\lesssim\sigma_1,\\
&\max\Big\{\big\|\mathbb{E}_{\boldsymbol{x}}[\boldsymbol{B}_3(\boldsymbol{x})^T\boldsymbol{B}_3(\boldsymbol{x})]\big\|_2,\big\|\mathbb{E}_{\boldsymbol{x}}[\boldsymbol{B}_3(\boldsymbol{x})^T\boldsymbol{B}_3(\boldsymbol{x})]\big\|_2\Big\}\lesssim K^2\sigma_1^2.
\end{aligned}\tag{115}$$

Define $\boldsymbol{Z}_{3,n}=\frac{1}{N}\big(\boldsymbol{B}_3(\boldsymbol{x}_n)-\mathbb{E}_{\boldsymbol{x}}\boldsymbol{B}_3(\boldsymbol{x})\big)$ for $(\boldsymbol{x}_n,y_n)\in\mathcal{D}$, and it is obvious $\boldsymbol{Z}_{3,n}$ is zero mean. Also, we have

$$\begin{aligned}
R_3=\|\boldsymbol{Z}_{3,n}\|_2\leq&\frac{1}{N}\big(\|\boldsymbol{B}_3(\boldsymbol{x}_n)\|_2+\|\mathbb{E}_{\boldsymbol{x}}\boldsymbol{B}_3(\boldsymbol{x})\|_2\big)\\
\lesssim&N^{-1}\sigma_1K^{\frac{3}{2}}\log^{\frac{5}{2}}d,
\end{aligned}\tag{116}$$

and

$$\begin{aligned}
\delta_3^2=\Big\{\Big\|\sum_{n=1}^{N}\mathbb{E}\boldsymbol{Z}_{3,n}\boldsymbol{Z}_{3,n}^T\Big\|_2,\Big\|\sum_{n=1}^{N}\mathbb{E}\boldsymbol{Z}_{3,n}\boldsymbol{Z}_{3,n}^T\Big\|_2\Big\}\leq&\frac{1}{N}\big(\|\mathbb{E}\boldsymbol{B}_3^2(\boldsymbol{x}_n)\|_2+\|\mathbb{E}\boldsymbol{B}_3(\boldsymbol{x}_n)\|_2^2\big)\\
\lesssim&N^{-1}K^2\sigma_1^2.
\end{aligned}\tag{117}$$

Similar to (108), by applying Lemma 10, we have

$$\Big\| \sum_{n=1}^{N} \boldsymbol{Z}_{3,n} \Big\|_2 \lesssim \sigma_1 \sqrt{\frac{K^2 \log d}{N}} \tag{118}$$

with probability at least $1 - d^{-10}$ provided that $N \gtrsim K^3 \log^6 d$.

Similar to (114), we define $\boldsymbol{B}$ by flattening the tensor $\sum_{n=1}^{N} \big[(\widehat{\boldsymbol{V}}^T \widetilde{\boldsymbol{x}})^{\otimes 3} - (\widehat{\boldsymbol{V}}^T \widetilde{\boldsymbol{x}}) \otimes (\mathbb{E}(\widehat{\boldsymbol{V}}^T \widetilde{\boldsymbol{x}})(\widehat{\boldsymbol{V}}^T \widetilde{\boldsymbol{x}})^T) \big]$ along the first dimension. Then, we know that

$$\begin{aligned} \|\boldsymbol{B}\|_2 \leq \Big\| \sum_{n=1}^{N} \widehat{\boldsymbol{V}}^T \widetilde{\boldsymbol{x}}_n \Big\|_2^3 + 3K \Big\| \sum_{n=1}^{N} \widehat{\boldsymbol{V}}^T \widetilde{\boldsymbol{x}}_n \Big\|_2 &\lesssim \Big(\frac{K \log d}{N} \Big)^{\frac{3}{2}} + 3K \Big(\frac{K \log d}{N} \Big)^{\frac{1}{2}} \\ &\lesssim \Big(\frac{K \log d}{N} \Big)^{\frac{1}{2}} + \Big(\frac{K^3 \log d}{N} \Big)^{\frac{1}{2}} \\ &\lesssim \sqrt{\frac{K^3 \log d}{N}}, \end{aligned} \tag{119}$$

provided that $N \gtrsim K \log d$.

In conclusion, we have

$$\Big\| \widehat{\boldsymbol{M}}_3(\widehat{\boldsymbol{V}}, \widehat{\boldsymbol{V}}, \widehat{\boldsymbol{V}}) - \boldsymbol{M}_3(\widehat{\boldsymbol{V}}, \widehat{\boldsymbol{V}}, \widehat{\boldsymbol{V}}) \Big\| \lesssim (\sigma_1 + |\xi|) \sqrt{\frac{K^3 \log d}{N}} \tag{120}$$

with probability at least $1 - d^{-C}$ provided that $N \gtrsim K^3 \log^6 d$.

□

I.3 Error bound for the first-order moment

Proof of Lemma 9. For $\widehat{\boldsymbol{M}}_1 - \boldsymbol{M}_1$, we have

$$\begin{aligned} \widehat{\boldsymbol{M}}_1 - \boldsymbol{M}_1 =& \frac{1}{N} \sum_{n=1}^{N} y_n \widetilde{\boldsymbol{x}}_n - \mathbb{E}_{\boldsymbol{x}}\, y \widetilde{\boldsymbol{x}} \\ =& \frac{1}{N} \sum_{n=1}^{N} \big(\frac{1}{K} \sum_{j=1}^{K} \phi(\boldsymbol{w}_j^{*T} \boldsymbol{x}_{n,\Omega_j}) + \xi_n \big) \widetilde{\boldsymbol{x}}_n - \mathbb{E}_{\boldsymbol{x}} \sum_{j=1}^{K} \frac{1}{K} \phi(\boldsymbol{w}_j^{*T} \boldsymbol{x}_{\Omega_j}) \widetilde{\boldsymbol{x}} \\ =& \frac{1}{K \cdot N} \sum_{j=1}^{K} \sum_{n=1}^{N} \Big(\phi(\boldsymbol{w}_j^{*T} \boldsymbol{x}_{n,\Omega_j}) \widetilde{\boldsymbol{x}}_n - \mathbb{E}_{\boldsymbol{x}}\, \phi(\boldsymbol{w}_j^{*T} \boldsymbol{x}_{\Omega_j}) \widetilde{\boldsymbol{x}} \Big) + \frac{1}{N} \sum_{n=1}^{N} \xi_n \cdot \widetilde{\boldsymbol{x}}_n. \end{aligned} \tag{121}$$

Define $\boldsymbol{B}_1(\boldsymbol{x}) := \frac{1}{K} \sum_{j=1}^{K} \phi(\boldsymbol{w}_j^{*T} \boldsymbol{x}_{n,\Omega_j}) \widetilde{\boldsymbol{x}}_n$, then we have

$$\begin{gathered} \|\boldsymbol{B}_1(\boldsymbol{x})\|_2 \lesssim \sigma_1 r \log^{\frac{3}{2}} d; \\ \|\mathbb{E}_{\boldsymbol{x}} \boldsymbol{B}_1(\boldsymbol{x})\|_2 \lesssim \sigma_1; \\ \Big\{ \big\| \boldsymbol{E}_{\boldsymbol{x}}[\boldsymbol{B}_1(\boldsymbol{x}) \boldsymbol{B}_1(\boldsymbol{x})^T] \big\|_2, \big\| \boldsymbol{E}_{\boldsymbol{x}}[\boldsymbol{B}_{1,j}(\boldsymbol{x})^T \boldsymbol{B}_1(\boldsymbol{x})] \big\|_2 \Big\} \lesssim \sigma_1^2. \end{gathered} \tag{122}$$

Next, define $\boldsymbol{Z}_{1,n} = \frac{1}{N} \big(\boldsymbol{B}_{1,j}(\boldsymbol{x}_n) - \mathbb{E}_{\boldsymbol{x}} \boldsymbol{B}_2(\boldsymbol{x}) \big)$ for $(\boldsymbol{x}_n, y_n) \in \mathcal{D}$, by calculation, we can obtain

$$R_1 = \|\boldsymbol{Z}_{1,n}\|_2 \lesssim N^{-1} \sigma_1 r \log^{\frac{3}{2}} d, \tag{123}$$

and

$$\delta_1^2 = \max\left\{ \left\| \sum_{n=1}^{N} \mathbb{E}\boldsymbol{Z}_{1,n}\boldsymbol{Z}_{1,n}^T \right\|_2^2, \left| \sum_{n=1}^{N} \boldsymbol{Z}_{1,n}^T \boldsymbol{Z}_{1,n} \right| \right\} \lesssim N^{-1}\sigma_1^2 r. \tag{124}$$

By applying Lemma 10, we have

$$\left\| \sum_{n=1}^{N} \boldsymbol{Z}_{1,n} \right\|_2 \lesssim \sigma_1 \sqrt{\frac{r \log d}{N}} \tag{125}$$

with probability at least $1 - d^{-10}$ provided that $N \gtrsim r \log^4 d$. Since $\boldsymbol{x} \in \mathbb{R}^r$ belongs to the Gaussian distribution, we have

$$\left\| \frac{1}{N} \sum_{n=1}^{N} \widetilde{\boldsymbol{x}} \right\|_2 \lesssim \sqrt{\frac{r \log d}{N}} \tag{126}$$

with probability at least $1 - d^{-10}$.

In conclusion, we have

$$\|\widehat{\boldsymbol{M}}_1 - \boldsymbol{M}_1\| \lesssim (\sigma_1 + |\xi|)\sqrt{\frac{r \log d}{N}} \tag{127}$$

with probability at least $1 - d^{-C}$, provided that $N \gtrsim r \log^4 d$. □